

Minerva Access is the Institutional Repository of The University of Melbourne

Author/s:

Billings, JL;Gordon, SL;Rawling, T;Doble, PA;Bush, AI;Adlard, PA;Finkelstein, DI;Hare, DJ

Title:

l-3,4-dihydroxyphenylalanine (l-DOPA) modulates brain iron, dopaminergic neurodegeneration and motor dysfunction in iron overload and mutant alpha-synuclein mouse models of Parkinson's disease

Date:

2019-07-01

Citation:

Billings, J. L., Gordon, S. L., Rawling, T., Doble, P. A., Bush, A. I., Adlard, P. A., Finkelstein, D. I. & Hare, D. J. (2019). l-3,4-dihydroxyphenylalanine (l-DOPA) modulates brain iron, dopaminergic neurodegeneration and motor dysfunction in iron overload and mutant alpha-synuclein mouse models of Parkinson's disease. *Journal of Neurochemistry*, 150 (1), pp.88-106. <https://doi.org/10.1111/jnc.14676>.

Persistent Link:

<https://hdl.handle.net/11343/285656>

PROF. ASHLEY I BUSH (Orcid ID : 0000-0001-8259-9069)

DR. DAVID I FINKELSTEIN (Orcid ID : 0000-0002-8167-4917)

DR. DOMINIC HARE (Orcid ID : 0000-0002-5922-7643)

Article type : Original Article

**L-DOPA modulates brain iron, dopaminergic neurodegeneration and motor dysfunction in iron overload and mutant alpha-synuclein mouse models of Parkinson's disease**

**Running title: Effects of L-DOPA in iron and alpha-syn models of PD**

*Jessica L. Billings,\* Sarah L. Gordon,† Tristan Rawling,‡ Philip A. Doble,§ Ashley I. Bush,\* Paul A. Adlard,\* David I. Finkelstein\* and Dominic J. Hare.\*§¶*

*\* Melbourne Dementia Research Centre at The Florey Institute of Neuroscience and Mental Health and The University of Melbourne, Parkville, Victoria, Australia.*

*† The Florey Institute of Neuroscience and Mental Health, Parkville, Victoria.*

*‡ School of Mathematical and Physical Sciences, Faculty of Science, University of Technology Sydney, Broadway, New South Wales, Australia.*

*§ Elemental Bio-imaging Facility, University of Technology Sydney, Broadway, New South Wales, Australia.*

*¶ Department of Clinical Pathology, The University of Melbourne, Parkville, Victoria, Australia.*

*Address correspondence and reprint requests to: Associate Professor Dominic J. Hare, The Florey Institute of Neuroscience and Mental Health, 30 Royal Parade, Parkville, Victoria 3052, Australia. Email: dominic.hare@florey.edu.au; or Associate Professor David I.*

**This is the author manuscript accepted for publication and has undergone full peer review but has not been through the copyediting, typesetting, pagination and proofreading process, which may lead to differences between this version and the [Version of Record](#). Please cite this article as [doi: 10.1111/JNC.14676](https://doi.org/10.1111/JNC.14676)**

This article is protected by copyright. All rights reserved

Finkelstein, The Florey Institute of Neuroscience and Mental Health, 30 Royal Parade, Parkville, Victoria 3052, Australia. Email: david.finkelstein@florey.edu.au

*Abbreviations: 3-MT, 3-methoxytyramine; 8-HQ, 8-hydroxyquinoline; AAAH, aromatic amino acid hydroxylases; AADC, aromatic L-amino acid decarboxylase; AADH, aromatic amine dehydrogenase; ALDH, aldehyde dehydrogenase;  $\alpha$ -syn,  $\alpha$ -synuclein; BSA, bovine serum albumin; CB, cerebellum; COMT, catechol-O-methyltransferase; CPu, caudate putamen; CQ, clioquinol; CTX, cortex; DA, dopamine; DAergic, dopaminergic; DBH, dopamine  $\beta$ -hydroxylase; DCF, dichlorofluorescein diacetate; DNP, dinitrophenyl; DNPH, 2,4-dinitrophenylhydrazine; DOPAC, 3,4-dihydroxyphenylacetic acid; DOPAL, 3,4-dihydroxyphenylacetaldehyde; HVA, homovanillic acid; L-DOPA, L-3,4-dihydroxyphenylalanine; LA-ICP-MS, laser ablation-inductively coupled plasma-mass spectrometry; NM, neuromelanin; LIP, labile iron pool; LPO, lipid peroxidation; PH, phenylalanine 4-hydroxylase; PNMT, phenylethanolamine N-methyltransferase; ROS, reactive oxygen species; SNc, substantia nigra pars compacta; SNr, substantia nigra pars reticulata; TH, tyrosine-3-hydroxylase; VTA, ventral tegmental area.*

**Abstract:**

Treatment with the dopamine (DA) precursor L-3,4-dihydroxyphenylalanine (L-DOPA) provides symptomatic relief arising from DA denervation in Parkinson's disease. Mounting evidence that DA autooxidation to neurotoxic quinones is involved in Parkinson's disease pathogenesis has raised concern about potentiation of oxidative stress by L-DOPA. The rate of DA quinone formation increases in the presence of excess redox-active iron (Fe), which is a pathological hallmark of Parkinson's disease. Conversely, L-DOPA has pH-dependent Fe-chelating properties, and may act to 'redox silence' Fe and partially allay DA autooxidation. We examined the effects of L-DOPA in three murine models of parkinsonian neurodegeneration: early-life Fe overexposure in wildtype (WT) mice, transgenic human (h)A53T mutant  $\alpha$ -synuclein ( $\alpha$ -syn) overexpression, and a combined 'multi-hit' model of Fe-overload in hA53T mice. We found that L-DOPA was neuroprotective and prevented age-related Fe accumulation in the substantia nigra pars compacta (SNc), similar to the mild-affinity Fe chelator clioquinol (CQ). Chronic L-DOPA treatment showed no evidence of increased oxidative stress in WT midbrain and normalised motor performance, when excess Fe was present. Similarly, L-DOPA also did not exacerbate protein oxidation levels in hA53T

mice, with or without excess nigral Fe, and showed evidence of neuroprotection. The effects of L-DOPA in Fe-fed hA53T mice were somewhat muted, suggesting that Fe-chelation alone is insufficient to attenuate neuron loss in an animal model also recapitulating altered DA metabolism. In summary, we found no evidence in any of our model systems that L-DOPA treatment accentuated neurodegeneration, suggesting DA replacement therapy does not contribute to oxidative stress in the Parkinson's disease brain.

**Keywords:**

alpha-synuclein, clioquinol, hA53T; iron, L-DOPA.

**Introduction**

Parkinson's disease is a progressive neurodegenerative disorder affecting neurons and the neural networks within the basal ganglia. The most severe neuropathology is seen within the substantia nigra pars compacta (SNc), where dopamine (DA) producing neurons are lost, resulting in denervation of nigrostriatal DA and resulting motor dysfunction. Parkinson's disease affects 1-2 per 1,000 of the global population, and 1% of all over the age of 60 years (Tysnes & Storstein 2017). There is no disease-modifying treatment currently in clinical use. While there are several candidate therapies in human trials, the diversity of known risk factors and resulting pathological targets highlight the difficulty in slowing progression of a disease for which there is no exact underlying cause in 80-85% of cases. In reality, these idiopathic Parkinson's disease cases likely include a range of genetic association and environmental factors such as air pollution-neuroinflammation (Lee *et al.* 2016) and neurotoxic pesticide exposure (Di Monte 2003) resulting in a spectrum of biochemical triggers, and consequently, therapeutic targets (Lang & Espay 2018).

L-3,4-dihydroxyphenylalanine, or levodopa (L-DOPA), is the primary precursor to DA that first showed clinical efficacy in alleviating motor symptoms in the 1960s (Birkmayer & Hornykiewicz 1961, Birkmayer & Hornykiewicz 1962, Cotzias *et al.* 1967) and remains the primary pharmacological treatment for Parkinson's disease symptoms. While L-DOPA therapy has improved the quality of life of tens of thousands of Parkinson's disease patients (Mercuri & Bernardi 2005), it has a significant side effect profile (Foster & Hoffer 2004). Although L-DOPA does provide some symptomatic relief in the period immediately

following onset of motor symptoms, during the later disease stages a number of non-L-DOPA-responsive symptoms emerge that contribute to the rapid decline in quality of life (Hely *et al.* 2005). A decade after diagnosis, symptom profiles of L-DOPA and non-treated Parkinson's disease patients are indistinguishable (Katzenschlager *et al.* 2008), suggesting that the therapy does not accelerate the symptoms of the condition. The question as to whether L-DOPA accelerates disease progression by potentiating neuron death is the subject of much debate (Lipski *et al.* 2011, Parkkinen *et al.* 2011).

There are several features common across all sporadic forms of the disease that are implicated in the underlying biochemical mechanism of disease that may be influenced by L-DOPA treatment, including: i) oligomerisation, aggregation, and deposition of alpha-synuclein ( $\alpha$ -syn) as Lewy pathology throughout the brain, including the SNc (Kalia & Lang 2016); ii) increased levels of oxidative stress (Jiang *et al.* 2016) in cells already maintaining a high basal oxidative load; and a SNc-specific accumulation of iron (Fe) beyond that of normal ageing (Ward *et al.* 2014, Ayton & Lei 2014). An emerging theory is that the unique chemical environment of DAergic neurons in the SNc is particularly susceptible to neurotoxic DA quinones formed by Fe-catalysed DA oxidation (Zucca *et al.* 2017, Hare & Double 2016), which also implicates  $\alpha$ -syn *via* its proposed regulation by Fe levels and role in vesicular transport of DA (Song & Xie 2018).

While it is acknowledged that no hard evidence directly links L-DOPA toxicity to neuron loss in Parkinson's disease patients, the uncertainty around this issue is a major contributor to the cautious approach that recommends the lowest dose providing symptomatic relief be applied (Olanow 2015). Clinical symptoms do not appear until 50% of SNc DAergic neurons have been lost, and up to 90% depletion has occurred within the first few years post-diagnosis (Kordower *et al.* 2013). This explains the loss of efficacy of L-DOPA in later stages of disease, though whether it contributes to the rate of neuron loss between diagnosis and near-total DA denervation remains unknown.

The proposed mechanism of L-DOPA-potentialiation of DA neurotoxicity is relatively straightforward (Fig. 1); therapeutic administration of a DA precursor to supplement depleted DA levels could, in theory, be contributing to oxidative stress by increasing the available pool of DA to oxidise (Herrera *et al.* 2017), particularly in the presence of excess reactive Fe (Sun *et al.* 2016). Iron has a high affinity to neuromelanin (NM) (Bohic *et al.* 2008), the

biopolymer formed by Fe-induced DA oxidation, and Fe is also a cofactor in several key enzymes involved in DA biosynthesis, including the two aromatic amino acid hydroxylases (phenylalanine 4-hydroxylase [PH] and tyrosine-3-hydroxylase [TH]) that produce endogenous L-DOPA from L-phenylalanine, and the haem-containing SNc-expressed cytochrome P450 2D6 (CYP2D6) enzyme that mediates the conversion of *p*-tyramine to DA following decarboxylation of L-tyrosine. Dopamine breakdown also relies on Fe catalysis; monoamine oxidase (MAO; primarily as the -B enzyme) activity is modulated by Fe (Lu *et al.* 2017) and is the enzyme used to deaminate DA to 3,4-dihydroxyphenylacetaldehyde (DOPAL) and 3-methoxytyramine (3-MT) to excretable homovanillic acid (HVA). Catechol-O-methyltransferase (COMT) is also central to HVA production by degrading DOPAL-derived 3,4-dihydroxyphenylacetic acid (DOPAC) to HVA, and DA to 3-MT. While X-ray crystallography studies of the COMT active site show no evidence of Fe-binding (Vidgren 1997), the mild-affinity Fe chelator 1,2-dimethyl-3-hydroxypyridin-4-one, or L1 was shown to inhibit COMT (and TH) activity in rats (Waldmeier *et al.* 1993). L-DOPA can readily cross the blood brain barrier (BBB) but must be delivered in combination with a DOPA decarboxylase inhibitor to prevent formation of BBB-impermeable DA outside the CNS. The pH dependent Fe-chelating properties of L-DOPA are well known, and it is advised that patients receiving oral treatment avoid Fe supplements that reduce uptake in the duodenum and jejunum (Campbell & Hasinoff 1989, Campbell *et al.* 1990).

Published reports of potential L-DOPA neurotoxicity in healthy DA neurons are conflicting; studies from the early 1980s failed to identify measurable damage to the nigrostriatal pathway in healthy rodents (Hefti *et al.* 1981, Perry *et al.* 1984), though numerous follow-up studies, reviewed in detail by Asanuma *et al.* (2003), suggest that chronic L-DOPA administration can, and does, promote DA oxidation and potentiate neuronal loss. It is important to note, however, that almost all our knowledge of potential L-DOPA neurotoxicity has been obtained from experiments using cell culture and lower-order species, often at supratherapeutic concentrations and chemical conditions (*e.g.* pH, dissolved O<sub>2</sub>, *etc.*) that do not reproduce the complex biochemistry of the diseased human brain. The Earlier versus Later Levodopa Therapy in Parkinson Disease (ELLDOPA) trial, designed specifically to investigate neurotoxicity of L-DOPA in humans, was inconclusive (Fahn *et al.* 2004). The subsequent Levodopa in EARly Parkinson's disease (LEAP) study (Verschuur *et al.* 2015) is currently underway (EudraCT number 2011-000678-72) and will add valuable new insight, though until conclusive evidence that L-DOPA is neurotoxic in humans is presented, it will

remain a front-line treatment for Parkinson's disease. Between these *in vitro* studies and clinical trials, murine models that recapitulate progressive iron accumulation, with dysfunctional  $\alpha$ -syn and impaired DA trafficking are the ideal testbed to test the hypothesis that L-DOPA accentuates DA neurotoxicity in a high-Fe environment.

Our group (Billings *et al.* 2016) and others (Kaur *et al.* 2007, Jia *et al.* 2018) have shown that increasing brain Fe accumulation *via* early-life dietary overexposure is sufficient to induce age-related nigrostriatal damage and parkinsonism, as evidenced by a specific loss of TH-positive neurons, increased markers of oxidative stress, and locomotor deficits measured as a decrease in spontaneous motor activity. Further, treatment with the Fe chelator clioquinol (5-chloro-7-iodo-quinolin-8-ol; CQ) from five months of age was able to prevent DAergic cell loss in Fe-loaded animals (Billings *et al.* 2016), attenuate the Fe-dependent neurotoxicity of 1-methyl-4-phenyl-1,2,3,6-tetrahydropyridine (MPTP) (Kaur *et al.* 2003, Hare *et al.* 2013a) and suppress the parkinsonian phenotype in mice overexpressing the human (h)A53T mutation to *SNCA* ( $\alpha$ -syn) (Finkelstein *et al.* 2016). Clioquinol has moderate affinity to Fe (Bareggi & Cornelli 2012) and by redox-silencing labile Fe it is thought to prevent excessive reactive oxygen species (ROS) formation (Dixon & Stockwell 2014). This has spawned a number of subsequent candidate compounds based on the 8-hydroxyquinoline (8-HQ) scaffold as possible agents for targeting metal-mediated neurodegeneration (Barnham & Bush 2014). Neurotoxicity of the hA53T mutation itself is accentuated by Fe (Ostrerova-Golts *et al.* 2000, Zhu *et al.* 2016), and we have previously hypothesised that permeable vesicles produced by mutant  $\alpha$ -syn 'leak' DA into the cytosol (Lotharius & Brundin 2002a) where it is free to react with labile Fe as it accumulates with age (Hare *et al.* 2017a, Hare *et al.* 2015).

Considering the substantial conflicts in the literature regarding whether L-DOPA is either neurotoxic or protective, and that Fe has multiple well-established roles in both normal DA metabolism and neurotoxic oxidation, we examined the effects of L-DOPA administration in three murine models of Parkinson's disease: early-life Fe overexposure to accelerated age-related accumulation (Kaur *et al.* 2007), hA53T overexpressing mice, which display disrupted DA metabolism (Giasson *et al.* 2002), and a dual-hit model combining the two experimental paradigms (Billings *et al.* 2016). We examined the *in vitro* Fe-redox-silencing properties of L-DOPA, spatial and total brain Fe levels, neuronal cell numbers, and motor function (all compared against CQ as a known Fe-chelator) to assess the specific effects of L-

DOPA on DA neurons and disease phenotype, prior to the equivalent onset of clinical symptoms. We found no compelling evidence that L-DOPA potentiates DAergic neurotoxicity when challenged with aberrant levels of Fe and dysfunctional A53T mutant human  $\alpha$ -syn but instead shows a slight capacity to mitigate the effects of the oxidative milieu of stressed neurons.

## Materials and Methods

### *Animal ethics approval and experimental design*

All experiments were in adherence to the National Health and Medical Research Council code for the care and use of animals for scientific purposes and were approved prior to commencement by the University of Melbourne Animal Ethics Committee (ID 08-023). A 2 x 4 factorial study design was used to determine the influences of a result (quantitative variable) based on two independent variables and appropriate animal numbers in SPSS v16 (IBM, USA). An interaction is the effect of one independent variable on a test (dependent variable) which relies on the value or the relationship of another independent variable. Interactions between neonatal iron supplementation and the type of treatment were investigated and analysed further using ANOVA together with the LSD *post hoc* test.

Experimental animals (equal ratio male to female) were born from pregnant wild type (WT) C57BL/6 or homozygous (+/+) hA35T mutant mice (B6;C3-Tg (Prnp-SNCA\*A53T)83Vle/J; A53T  $\alpha$ -synuclein transgenic line M83; RRID:IMSR\_JAX:004479, Jackson Laboratories, USA), who were housed at a constant temperature of 22 °C in a 12-hour light/dark cycle. Mothers had access to water and standard rodent chow (Glenforrest Stockfeeders, Australia) *ad libitum*. Experimental groups and dosing regimen are shown in Figure 2. Each animal was assigned a random identifier using the random number generator function in Microsoft Excel (Microsoft Corporation, USA) and experimenters were blinded to sample groups until after analysis.

### *Hydrogen peroxide assay*

The ability of L-DOPA and CQ to inhibit Fe-mediated production of hydrogen peroxide ( $H_2O_2$ ) was measured using a modified indirect fluorescence detection assay (Finkelstein *et*

*al.* 2017, Opazo *et al.* 2002). Dichlorofluorescein diacetate (DCF; Molecular Probes, USA) was dissolved in dimethyl sulfoxide (DMSO; Sigma Aldrich) to a concentration of 5 mM in an argon-purged atmosphere. Sodium hydroxide (0.25 M) was added to deacetylate the DCF for 30 min, after which the solution was pH-adjusted to 7.4 for a final DCF concentration of 0.1 mM. A 0.1  $\mu$ M solution of horseradish peroxidase (HRP; Sigma Aldrich) was prepared in 0.1 M phosphate buffered saline (PBS) at pH 7.4. Reagents were added to a 96-well plate and the reaction proceeded at 37 °C in a light-free environment to prevent photodynamic interference. All experiments used a constant Fe concentration (as ferric ammonium citrate; Sigma Aldrich) of 400 nM and 10  $\mu$ M ascorbate was included as a reducing agent in all samples. Fluorescence measurements were recorded on a Perkin Elmer LS-55 fluorometer with excitation and emission wavelengths of 485 nm and 530 nm, respectively.

#### *Genotyping of hA53T mice*

Mice tail biopsies were collected and homogenised in an extraction and preparatory buffer (REExtract-N-AMP Tissue PCR kit, Sigma, USA). Genotyping was performed by polymerase chain reaction (PCR) with  $\alpha$ -syn primers (forward: 5'-TGTAGGCTCCAAACCCAAGG-3'; reverse: 5'-TGTAGGCTCCAAACCCAAGG-3'; Sigma, USA) and run on a 1.5% agarose gel (Fig. S1). Samples were run in parallel with a confirmed <sup>+/+</sup>hA53T transgenic mouse standard and 100 bp molecular weight marker (NEB, USA).

#### *Early-life iron exposure*

*Post-natal* Fe feeding experiments were performed using the method previously described (Billings *et al.* 2016). Carbonyl Fe is a common food additive and was selected over ferrous salts as it is better tolerated while still providing a bioavailable source of Fe (Gordeuk *et al.* 1986). Carbonyl iron was suspended in an 8% (w/v) sucrose solution (CAS ID 7439-89-6; Sigma-Aldrich, Australia). Animals were delivered either Fe or vehicle solutions orally by dispensing the calculated dose from a syringe into the rodent's mouth from P10-P17 days of age. Animals received a daily dose of 0.12 mg kg<sup>-1</sup> Fe (or equivalent volume of vehicle), calculated daily according to weight of the pup. Iron dose was based on that devised by Kaur *et al.* (2007) and previously used by us (Billings *et al.* 2016) as a mimetic of typical commercial infant formula preparations that we have previously commented on as a potential

risk factor for brain iron accumulation (Hare *et al.* 2018) and Parkinson's disease (Hare *et al.* 2015, Hare *et al.* 2017a). Pups were housed with their mothers for the duration of Fe feeding. At 3 months of age body weights of vehicle and Fe-fed animal from both WT and hA53T strains ( $n = 5$  per group) were measured for seven days. Fe-feeding has no effect on total body weight (Fig. S2).

#### *Clioquinol and L-DOPA administration*

Clioquinol (Fig. 1, inset; CAS ID 130-26-7; Sigma-Aldrich) was administered to animals *via* supplemented rodent chow. Based on previous reports of efficacious CQ doses of  $\sim 30$  mg/kg for brain metal modulation in mice (Kaur *et al.* 2003, Cherny *et al.* 2001), we spiked GR2 rat and mouse pellets (Glenforrest Stockfeeders, Australia) with  $250 \text{ mg kg}^{-1}$  CQ and mixed thoroughly. To determine the mean daily intake of CQ by a 12-week-old C57BL/6 wild type mouse we measured the difference in mass of pellets daily for 10 days and calculated the mass-corrected intake as  $37 \text{ mg kg}^{-1}$  of CQ per day (Fig. S3). Mice were maintained on this diet from 3 to 8 months, after which they were culled.

L-DOPA (CAS ID 59-92-7; Sigma-Aldrich) administration was adapted from the previously published method by Parish *et al.* (2002). L-DOPA was delivered to mice in drinking water with 0.2 % (w/v) ascorbic acid and replaced every second day to limit oxidation. Drinking water was spiked with  $20 \text{ mg L}^{-1}$  of the aromatic L-amino acid decarboxylase (AADC) inhibitor benserazide (Fig. 1, inset; CAS ID 14919-77-8; Roche, Australia) to limit L-DOPA to DA conversion in the peripheral nervous system. Dose was calculated based on a 30 g mouse consuming 3 mL of water per day, which was equivalent to a daily oral dose of  $20 \text{ mg kg}^{-1}$  L-DOPA and  $2 \text{ mg kg}^{-1}$  benserazide. Animals receiving combined CQ and L-DOPA were exposed as outlined above. Each treatment group were housed in separate enclosures. While we acknowledge that dose control using food and drinking water is less precise than oral gavage, due to the 5-month duration of chronic exposure it was decided that gavaging would cause undue stress to the animals. L-DOPA dosing followed the same CQ treatment routine, commencing at 3 months and continuing until culling at 8 months. Vehicle-treated animals received drinking water with 0.2% (w/v) ascorbic acid only.

The ranges and routes of administration for L-DOPA and benserazide dose vary across the literature and typically focus on single dose pharmacokinetics; in our study oral (p.o.)  $20 \text{ mg}$

kg<sup>-1</sup> L-DOPA with 2 mg kg<sup>-1</sup> benserazide in drinking water was a suitable chronic dose choice as it had minimal effect over an extended treatment paradigm with no apparent adverse physical effects. Intraperitoneal (i.p.) administration of benserazide is problematic due to concerns that nigrostriatal AADC activity is also inhibited by high BBB-permeable doses; a high i.p. dose of benserazide (50 mg kg<sup>-1</sup>; 25 times the daily p.o. dose used here, in a single injection) in rats has been previously reported to increase AADC activity and extracellular striatal DA *prior* to administration of L-DOPA (25 mg kg<sup>-1</sup> i.p.) 30 minutes later. Lowering the dose to 10 mg kg<sup>-1</sup> decreased striatal AADC activity though not DA levels until after L-DOPA administration (Jonkers *et al.* 2001). High benserazide (50 mg kg<sup>-1</sup> i.p.) also increases levels of the DOPAC metabolite, though not HVA (de Silva *et al.* 1997). This raises important questions about off-target effects of AADC inhibitors, or an expanded role of the AADC enzyme in DA metabolism worthy of future study. The substantially lower oral dose used here, with gastrointestinal bioavailability of 66-74% (Ashley & Dunleavy 2017), was unlikely to have an inhibitory effect on nigrostriatal AADC activity. Oral doses of ~15 mg kg<sup>-1</sup> (7.5 times that used here) have been shown to have no effect on midbrain AADC activity (Prada *et al.* 1987). To our knowledge, unlike acute administration of parkinsonian neurotoxins like 6-OHDA (Carvey *et al.* 2005), there is no evidence that Fe-overload or hA53T expression induces increased BBB permeability, and thus benserazide uptake into the brain. There is evidence of BBB disruption in *post mortem* Parkinson's disease human striatal tissue (Gray & Woulfe 2015), yet whether this is a cause-or-effect of the disease cannot be determined from end-stage samples.  $\alpha$ -Syn is BBB-permeable, although interactions between the protein and BBB, reviewed in Bates and Zheng (2014), do not appear to influence barrier integrity. While a BBB-disrupting effect of benserazide cannot be discounted over the three-month course of treatment, the low dose and clinically-relevant oral route of administration was chosen to minimise this potential confounding effect.

### *Tissue collection*

At 8 months of age, animals were deeply anaesthetised with 100 mg kg<sup>-1</sup> sodium pentobarbitone (CAS ID 76-74-4; Lethobarb, Virbac, Australia) and had the thoracic cavity opened to expose the heart. The right atrium was cut and 25 mL of cold PBS (0.1 M; pH 7.4) with 0.5% (v/v) butylated hydroxytoluene to prevent additional oxidative changes to protein carbonyls was delivered *via* a peristaltic pump and 23-gauge needle inserted into the left ventricle. Once perfusion was complete, brains were removed and snap-frozen on dry ice,

then stored at -80 °C until required. All procedures were performed in accordance with the National Health and Medical Research Council (2008) and University of Melbourne Animal Care & Use Standards.

Whole intact brain regions were dissected using a chilled stainless-steel mouse brain matrix (Plastics One Inc., USA). Brains were aligned with the ventral side exposed and then dissected using the optic chiasm as a point of reference. Tissue from the caudate putamen (CPu), cortex (CTX; encompassing the primary/secondary motor cortices and somatosensory cortex), the midbrain containing the substantia nigra pars compacta (SNc) and pars reticulata (SNr) and cerebellum (CB) was immediately transferred to metal-free 1.5 mL polypropylene vials (Techno Plas, Australia) and stored at -80 °C.

#### *Inductively coupled plasma-mass spectrometry*

The Fe concentration in excised tissue was determined using inductively coupled plasma-mass spectrometry (ICP-MS). Samples were accurately weighed to obtain the wet tissue weight and then lyophilised overnight in a SpeedVac freeze drier (Dyna Vac, Australia). Based on tissue weight, 100-300 µL of 65% nitric acid (HNO<sub>3</sub>; Suprapur grade; Merk, Australia) was added to the lyophilised sample, which was then heated at 90 °C on a heating block for 20 min. When returned to room temperature, an equivalent volume of 30% H<sub>2</sub>O<sub>2</sub> (BDH, UK) was slowly added and left to digest for 30 minutes. Samples were then reheated to 70 °C for 15 min. The reduced volume was accurately measured and three 40 µL aliquots were diluted to 1 mL in 1% (v/v) HNO<sub>3</sub>. Blanks of each solvent and digestion blanks were collected at regular intervals, and suitable analytical recovery ( $\pm 10\%$  of certified value) was measured using digested lyophilised bovine liver (SRM 1577b, National Institute of Standards and Technology, USA).

All samples were analysed using a Varian UltraMass 700 (Agilent Technologies, Australia), externally calibrated using a blank and 10, 50 and 100 µg L<sup>-1</sup> solutions prepared from a certified multi-element ICP-MS standard solution (CA2-1; Accustandard, USA) diluted in 1% HNO<sub>3</sub>. A 100 µg L<sup>-1</sup> solution of yttrium in 1% HNO<sub>3</sub> (IS-MIX1-1, Accustandard) was introduced online *via* a Teflon T-piece and used as an internal standard for all measurements. Results from the ICP-MS analysis of the triplicate samples were averaged and then corrected

for both reduced volume and sample weight, with a final concentration reported at  $\mu\text{g g}^{-1}$  of wet weight tissue.

### *Tissue sectioning*

Extracted brains for cytometry were cryoprotected following our previously published methods to minimise loss of Fe (Hare *et al.* 2013b). Briefly, brains were placed in a solution of 4% (w/v) paraformaldehyde (PFA; Sigma Aldrich) in 0.2 M PBS (pH 7.4) and left overnight to fix at 4 °C. Brains were then passed through two changes of 30% (w/v) sucrose solution in 0.2 M PBS (pH 7.4) before being frozen on dry ice and stored at -80 °C prior to sectioning.

Brains were mounted in optimal cutting temperature compound (OTC; ProSciTech, Australia) and sectioned at -20 °C on a Leica cryostat. Tissue was collected in a series of three, with 30  $\mu\text{m}$  thick sections mounted on gelatine-coated slides from the anterior to posterior of the SNc. Sections were stored at -80 °C prior to use.

### *Laser ablation-inductively coupled plasma-mass spectrometry imaging*

Imaging spatial Fe distribution was performed using laser ablation-inductively coupled plasma-mass spectrometry (LA-ICP-MS); see (Hare *et al.* 2017b) for a visual tutorial. Sections were retrieved from -80 °C and dried in a desiccator prior to analysis. A NewWave Research UP213 LA system (Kennelec Scientific, Australia) coupled to an Agilent Technologies 7500s Series ICP-MS (Agilent Technologies, Australia) was used for all experiments. Quantitative data was obtained by representative ablation of prepared matrix-matched tissue standards (Hare *et al.* 2013c), and hydrogen was used as a reaction gas to remove  $^{40}\text{Ar}^{16}\text{O}^+$  interference on  $^{56}\text{Fe}^+$  (Lear *et al.* 2012b). Laser parameters were selected to obtain final images with a spatial resolution of  $30 \times 30 \mu\text{m}$  (total pixel area =  $900 \mu\text{m}^2$ ) by rastering a 213 nm 20 Hz laser pulse with a diameter of 30  $\mu\text{m}$  across the sample at  $120 \mu\text{m s}^{-1}$  (Lear *et al.* 2012a). Images were constructed using ENVI (v5.3; Esri, Australia) (Hare *et al.* 2009). Regions of interest were selected by freehand drawing with the aid of our previously reported anatomical atlas of metal distribution in the C57BL/6 mouse brain (Hare *et al.* 2012).

## *Detection of protein carbonyls*

Protein carbonyls (C=O) are a product of oxidative damage and can be used as a marker of oxidative stress by derivatising to dinitrophenylhydrazone (DNP-hydrazone) with 2,4-dinitrophenylhydrazine (DNPH) (Dalle-Donne *et al.* 2003). DNP-hydrazone can then be detected and quantified by immunoblotting, in this case with an OxyBlot™ Protein Oxidation Detection Kit (Millipore, Australia). Weighed aliquots of fresh frozen tissue in 1.5 mL polypropylene tubes were homogenised using a sonicator blade (Branson Sonifer 450, 1/8 inch microtip taper blade, Australia) for one to two pulses and one 30 s rest period in a buffer containing calcium and magnesium-free Dulbecco's PBS (Sigma Aldrich) and EDTA-free protease inhibitor (Roche, Australia). Five times the tissue weight (*e.g.* 0.2 g per mL of buffer) was added to each sample, which was homogenised on ice. Following homogenisation, 0.5 M butylated hydroxytoluene (BHT; 2,6-bis(1,1-dimethylethyl)-4-methylphenol; Sigma Aldrich) in 1 mL acetonitrile (Scharlau, Spain) was added to quench further oxidation events. Samples were then centrifuged at 10000 *g* for 5 min at 4 °C and the supernatant removed for further analysis. Total protein content was measured using a BCA assay and all samples were diluted in duplicate in PBS to a standard 10 µg µL<sup>-1</sup> concentration before deionised water was added to make a final volume of 5 µL. An equal volume of 12% sodium dodecyl sulfate (SDS) was then added. Per manufacturer's instructions, 10 µL of DNPH solution was added to one aliquot and 10 µL of derivatisation control solution to the other. Samples were allowed to incubate at room temperature for 15 minutes, after which 7.5 µL of the neutralising solution was added.

Neutralised samples were then transferred to a nitrocellulose membrane for dot-blotting (BioRad, Australia). The membrane was blocked at room temperature in 1% bovine serum album (BSA) in PBS and Tween-20 (PBS-T) for 1 h with gentle agitation, after which a primary rabbit anti-DNP antibody solution (1:150 in BSA/PBS-T; RRID: AB\_10850321; Millipore) was added and incubated for a further 1 h. After rinsing twice and washing for 15 min with PBS-T, an HRP-conjugated goat anti-rabbit secondary antibody (1:300, BSA/PBS-T; RRID: AB\_11212848; Millipore) was added and the membrane incubated again for 1 h at room temperature. After final washing with PBS-T the membrane was covered in sufficient volume of supplied two-component chemiluminescent reagents (mixed in equal volumes immediately prior to use) for 1 min and then transferred to a fluorescence imaging system (FujiFilm, Japan) for analysis.

To determine the concentration of protein carbonyls, 2.5  $\mu\text{L}$  of an internal standard containing proteins with one to three DNP residues (equivalent to 100 fmoles) was run in parallel to each sample. Fluorescence from analysed samples was background corrected for PBS and extrapolated from the internal standard. Using the initial tissue mass, protein carbonyls were calculated as fmoles  $\mu\text{g}^{-1}$  of total tissue.

#### *Tyrosine hydroxylase immunohistochemistry*

For the first series of sections, slides were dried and brought to room temperature before being fixed in 4% PFA for approximately 30 seconds. After being rinsed in triplicate in tris-buffered saline and Tween-20 (TBS-T) the sections were blocked for 15 minutes in a 3% (v/v) normal goat serum (NGS) in TBS-T solution, then incubated at room temperature overnight with a 1:3000 dilution of polyclonal tyrosine hydroxylase (TH) antibody (AB152; RRID: AB\_390204; Millipore). Sections were rinsed again and incubated with an HRP-conjugated polyclonal goat-anti-rabbit secondary antibody (RRID: AB\_11212848; Millipore) for 1 hour at room temperature. Tyrosine hydroxylase staining was visualised with cobalt- and nickel-enhanced diaminobenzidine (DAB; Sigma Aldrich), after which sections were counterstained with neutral red, dehydrated, cleared and coverslipped.

#### *Cytometry*

Counting of TH-positive and TH-negative neurons was performed using a stereological fractionator design previously described (Finkelstein *et al.* 2000, Parish *et al.* 2002). The SNc was observed at  $10\times$  magnification and TH-positive neurons within this brain region were differentiated from TH-positive neurons in the adjacent ventral tegmental area (VTA) according to soma diameter (TH-SNc =  $16\ \mu\text{m}$ ; TH-VTA =  $13\ \mu\text{m}$ ). Both TH-positive and TH-negative neurons (*i.e.* neutral red-stained) within the SNc were scored. Using the optical fractionator rules (Gundersen *et al.* 1988), approximately 8 sections per animal were randomly selected from an arbitrary starting point. Cell counts were taken using an unbiased counting frame measuring  $35\times 45\ \mu\text{m}$  ( $1,575\ \mu\text{m}^2$ ) at regular intervals on a sampling grid of  $140\times 140\ \mu\text{m}$ . Cell counts were estimated using the Stereo Investigator software (Microbrightfield, USA) with a  $60\times 1.3$  N.A. oil objective lens.

### *Pole test*

The pole test is commonly used to assess movement dysfunction arising from DA denervation in mice (Matsuura *et al.* 1997). Mice were positioned with their heads facing upwards at the top end of a vertical rough surfaced 50 cm long, 1 cm diameter pole placed in their home cage. Animals were habituated to the pole 24-hours prior to testing and were allowed five consecutive trials. Animals were assessed for the fastest time taken to completely turn towards the home cage (T-turn) and the fastest total time needed to descend down the pole (T-total) of the five trials. If the mouse had either failed to turn completely or fell off the pole, default values were assigned (*i.e.* 60 s, and 120 s, respectively). Times were recorded by analysing digital video of the task. The scoring of each trial was analysed frame by frame (30 ms per frame) using Media Player Classic (Microsoft, USA) to ensure that the animals' hind limbs had completely rotated their grip (T-turn) and touched the base of the pole (T-total).

### *Statistics*

All statistical analyses were performed in Prism (v6; GraphPad, USA). Tests used included two-tailed Student's *t*-test for single variable comparisons, or one-way ANOVA with Fisher's least squares difference (LSD) *post hoc* testing for multiple independent comparisons against vehicle and Fe-fed groups. Outliers were removed using the ROBust regression and OUTlier removal (ROUT) method in Prism. Statistical significance was set at  $\alpha < 0.05$ .

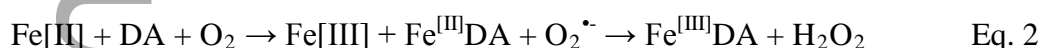
### *Data reproduction statement*

Aspects of this study include the use of data previously published by our group (Billings *et al.* 2016); specifically, data from non-L-DOPA-treated animals. All experiments using L-DOPA were performed parallel to other treatment groups. Data is reproduced with permission from the American Chemical Society *via* an ACS AuthorChoice Usage Agreement.

## **Results**

### *L-DOPA and CQ inhibit Fe-mediated production of H<sub>2</sub>O<sub>2</sub> in vitro*

Intracellular H<sub>2</sub>O<sub>2</sub> concentration is typically in the low μM range and varies depending on cell type (Weinstain *et al.* 2014), with extracellular concentrations around 10-fold higher (Kulagina & Michael 2003). Under physiological conditions, Fe catalyses decomposition of mitochondrially-produced H<sub>2</sub>O<sub>2</sub> to the superoxide radical (O<sub>2</sub><sup>•-</sup>). Iron is primarily redox-cycled between the +2 and +3 oxidation states *via* the Fenton and Haber-Weiss reactions (Papanikolaou & Pantopoulos 2005), allowing small amounts of labile Fe[II] to continually produce ROS unless redox-silenced by endogenous chaperones (*e.g.* ferritin (James *et al.* 2015)) or chelators like CQ (Kaur *et al.* 2003). Labile Fe[II] in aerobic conditions can also produce H<sub>2</sub>O<sub>2</sub> independent of mitochondrial respiration (Eq. 1), which is accelerated in the presence of DA by forming an unstable intermediary complex (Eq. 2) at pH 7.4 (Sun *et al.* 2018b, Sun *et al.* 2016):



As a structurally similar catecholamine, we used this *in vitro* measure to assess whether L-DOPA similarly increased ROS production in the presence of Fe and a reducing agent, or if Fe[II/III] chelating properties reported for L-DOPA (Rajan *et al.* 1978) attenuate H<sub>2</sub>O<sub>2</sub> production, compared against the mild-affinity Fe chelator CQ.

Redox-silencing by Fe chelation inhibits H<sub>2</sub>O<sub>2</sub> production and decreases measured DCF fluorescence. Estimated concentrations of H<sub>2</sub>O<sub>2</sub> were calculated using linear regression analysis of a three-point calibration curve derived from measured DCF fluorescence in 0 (as PBS), 1.0 and 2.5 μM H<sub>2</sub>O<sub>2</sub> standards (Fig. 3; Fig. S4). 400 nM Fe produced ~1.5 μM H<sub>2</sub>O<sub>2</sub>, with both 10 μM and 20 μM (both *p* < 0.001) CQ decreasing H<sub>2</sub>O<sub>2</sub> concentration by 39-46%. 10 μM L-DOPA had no increasing influence on Fe-mediated H<sub>2</sub>O<sub>2</sub> production, nor did it reduce the amount of detectable H<sub>2</sub>O<sub>2</sub> produced by spontaneous Fe oxidation (*p* = 0.9). 20 μM L-DOPA did, however, reduce H<sub>2</sub>O<sub>2</sub> to levels equivalent of 10 and 20 μM CQ (*p* < 0.001; Fig. 3).

*Evidence for L-DOPA modulation of nigrostriatal iron levels*

In both WT and hA53T transgenic mice early-life Fe exposure resulted in a specific increase in midbrain (including both SNc and SNr) Fe at 8 months (WT +18%; hA53T +48%; both  $p < 0.05$ ; Fig. 4a) that was ameliorated in both strains by chronic CQ ( $p < 0.001$ ) and L-DOPA ( $p < 0.05$ ) administration. Although the magnitude of midbrain Fe elevation was higher in hA53T transgenics ( $13.60 \pm 0.57$  vs  $17.46 \pm 9.19 \mu\text{g g}^{-1}$  wet tissue weight), midbrain Fe levels did not significantly differ between groups, which may be obscured by high variance in the hA53T animals. In the CPu, which receives projections from the SNc, early-life exposure did not significantly increase Fe levels ( $p = 0.5$ ; Fig. 4b), though CQ and L-DOPA treatment in the absence of Fe loading reduced CPu Fe concentration by -15% and -17% vs control, respectively (both  $p < 0.01$ ). Neither compound affected CPu Fe concentration in exposed animals, though Fe exposure combined with CQ and L-DOPA treatment reduced Fe by -15% compared to both control and Fe-fed mice (both  $p < 0.01$ ). In hA53T animals, CPu Fe concentration was more variable, and one-way ANOVA revealed no significant difference between treatments ( $p = 0.5$ ). Iron levels in the CTX and CB were unchanged (Fig. S5).

To examine how early-life Fe exposure influences neuroanatomical distribution of Fe at the mesoscale and possible redistribution effects of L-DOPA, we used LA-ICP-MS imaging to visualise and quantify the Fe content of the SNc in vehicle, Fe-fed and L-DOPA-treated WT animals. The SNc has an approximate volume of  $800 \times 1150 \mu\text{m}$  (Baquet *et al.* 2009) and cannot be easily dissected, thus midbrain tissue also contained the Fe-rich SNr and the VTA, which contains DA neurons with subtle biochemical differences compared to those in the SNc (Sulzer 2007), including markedly lower levels of Fe (Hare *et al.* 2014). While these neurons degenerate in Parkinson's disease, it occurs to a lesser extent than the SNc (Alberico *et al.* 2015) and at a later disease stage (Surmeier *et al.* 2017). Additional midbrain nuclei with lower Fe levels may therefore dilute or obscure regional accumulation of Fe following early-life exposure.

LA-ICP-MS confirmed that the observed increase in midbrain Fe was attributable to accumulation in the SN (Fig. 5a-c), with Fe-fed animals showing a 23% increase compared to control ( $p < 0.05$ ). Treatment with L-DOPA lowered SN Fe levels by 41% vs Fe-fed animals ( $p < 0.001$ ), 27% lower than vehicle ( $p < 0.05$ ; Fig. 5d).

*L-DOPA attenuates iron-mediated oxidative stress in the substantia nigra pars compacta*

Detection of protein carbonyls is a robust marker of oxidative stress resulting from both  $\alpha$ -syn and DA toxicity (Lotharius & Brundin 2002b). As expected from our previously reported results (Billings et al. 2016), protein carbonyls were increased twofold in the midbrain of Fe-loaded WT mice (+51%;  $p < 0.001$ ; Fig. 6a,b). Animals exposed to chronic L-DOPA in the absence of early-life Fe exposure showed no evidence of increased protein carbonyls ( $p = 0.8$ ), suggesting supplemental L-DOPA at the dose given does not promote downstream production of neurotoxic DA oxidation products at basal Fe levels. Iron-loaded mice exposed to chronic CQ, L-DOPA and the combined dosing regimen showed protein carbonyl levels equivalent to vehicle ( $p = 0.3-0.7$ ). As control animals for both WT and hA53T groups had substantially different baseline levels of protein carbonyls, comparisons between genotype are not possible. Protein carbonyl concentrations in hA53T mice were, as a whole, approximately half that observed in WT animals, with a counter-intuitive decrease in Fe-loaded hA53T mice ( $p < 0.05$ ) and higher variance in all measurements (Fig. 6c). We believe this is a strain effect that may be attributable to the differential downstream expression of multiple proteins in cells transfected with hA53T (Pennington *et al.* 2010), though a larger cohort would be needed to confirm this hypothesis.

#### *Combined chronic co-administration of CQ and L-DOPA may be neuroprotective*

Cell counting studies were performed using TH as a DAergic marker and neutral red to identify non-TH-positive neurons (Fig. 7) to examine possible neuroprotective effects of L-DOPA and CQ. Iron-loading in WT animals resulted in a significant decrease in total SNc neurons at 8 months (-26%,  $p < 0.001$ ; Fig. 8a). As previously reported, CQ-treated animals showed no significant neurodegeneration compared to control (Billings et al. 2016), nor did both L-DOPA and combined CQ + L-DOPA treated animals. Both L-DOPA and CQ-treated hA53T animals had comparable SNc neuron numbers to WT ( $p = 0.3-0.4$ ; Fig. 8b). Elevated levels of midbrain Fe did not potentiate hA53T neurotoxicity ( $p = 0.7$ ), though neither treatment alone recapitulated the effect observed in non-Fe-exposed transgenic mice ( $p = 0.06-0.1$ ). However, Fe-fed animals receiving concurrent administration of L-DOPA and CQ retained nigral neuronal populations comparable to WT ( $p = 0.5$ ).

As TH is the rate-limiting enzyme in DA synthesis (Daubner *et al.* 2011), we used this marker to stratify neurons in the SNc as TH-positive (*i.e.* DAergic) and TH-negative. Doing so revealed the varying effects of L-DOPA and CQ on DA-specific neuronal populations in

hA53T mice. The high degree of variance in hA53T neuronal numbers could be attributed to TH-positive neurons only. Surprisingly, Fe-loaded animals had 28% more DAergic neurons than vehicle-fed hA53T ( $p < 0.05$ ; Fig. 8c), while the SNc of L-DOPA and CQ-treated hA53T animals with no Fe loading contained 56% (equivalent to WT control;  $p = 0.6$ ) and 43% more TH-positive cells (-11% vs WT control,  $p < 0.05$ ) than vehicle-treated hA53T, respectively (both  $p < 0.001$ ). This effect was replicated in the Fe + L-DOPA and combined Fe-fed, L-DOPA and CQ-treated groups (+46% and +55% vs hA53T;  $p < 0.001$ ).

#### *L-DOPA and CQ attenuate pole test motor deficits in Fe overloaded animals but not hA53T mice*

Results from pole testing performed at  $t = 3, 4$  and 5 months ( $n = 4-6$  animals per group) showed a significant deterioration in motor function (as time-to-turn) in Fe-fed WT animals at 5 months (+95% vs vehicle;  $p < 0.001$ ; Fig. 9a) that was markedly attenuated by L-DOPA (+56% vs Fe-fed;  $p < 0.001$ ) and combined L-DOPA and CQ treatment (+51 vs Fe-fed;  $p < 0.01$ ), and to a lesser extent by CQ alone (+39% vs Fe-fed;  $p < 0.05$ ). Interestingly, mice treated with L-DOPA alone, or in combination with Fe (in presence or absence of CQ) displayed a faster time to complete the task (T-total) than WT (36-40% faster;  $p < 0.01$ ).

In the hA53T groups, variance was again high, and the only significant effect observed was in the time-to-turn in combined L-DOPA and CQ-treated animals compared to the hA53T vehicle group ( $p < 0.01$ ; Fig. 9b), though again data should be interpreted with caution. No obvious benefit of L-DOPA or CQ administration in hA53T Fe-fed animals was observed.

## **Discussion**

Nigral Fe accumulation is an early-stage disease event in Parkinson's disease (He *et al.* 2015). Given that under healthy conditions DAergic neurons in the SNc maintain an elevated basal Fe levels, owing to their high metabolic output and multiple Fe-dependent functions, these cells would logically be susceptible to increased pro-oxidant activity and accordingly have greater transcription levels of key antioxidant proteins (Hare *et al.* 2014). These including superoxide dismutase-1 (itself having impaired function in Parkinson's disease (Trist *et al.* 2017)), DJ-1 (Biosa *et al.* 2017) (also involved in 20S-proteasome regulation (Moscovitz *et al.* 2015)), and a deficient glutathione system (Sian *et al.* 1994, Seibt *et al.*

2018). There is compelling evidence that an oxidative cascade triggered by aberrant reactions between Fe, DA, and  $\alpha$ -syn is a possible pathogenic event occurring long before overt neurodegeneration and manifestation of clinical symptoms, and Fe accumulation is recognised in the research criteria for prodromal (asymptomatic) Parkinson's disease (Berg *et al.* 2015). Overexpression of  $\alpha$ -syn, as WT type or human mutant variants (Giasson *et al.* 2002, Chesselet 2007, Fleming *et al.* 2004) and excess Fe levels (Sobotka *et al.* 1996, Fredriksson *et al.* 1999, Kaur *et al.* 2007, Fredriksson *et al.* 2001) confers an associated risk of both preclinical and neuropathological parkinsonism in mice models. When combined, previously-reported neuroprotective effects of a mild Fe-chelator in each individual paradigm is lost (Billings *et al.* 2016, Finkelstein *et al.* 2016).

The primary concern of Fe-mediated oxidation of both L-DOPA and DA is the production  $H_2O_2$ , which quickly degrades to damaging hydroxyl radicals (Lai & Yu 1997) *per* the Fenton and Haber-Weiss process. However, concurrently-formed DA quinones are acutely neurotoxic, having confirmed negative effects on mitochondrial function,  $\alpha$ -syn fibrilisation, proteasomal and lysosomal function, and a direct contribution to oxidative stress (Segura-Aguilar *et al.* 2014). L-DOPA and DA were shown to suppress lipid peroxidation (LPO) *ex vivo*, both in the presence and absence of  $Fe^{3+}$ , though when a reducing agent was added LPO products dramatically increased (Li *et al.* 1995), suggesting an Fe[II]-dependent process and supported *in vitro* studies demonstrating increased DA quinones production in a Fe-rich reducing environment (Sun *et al.* 2018a). Both Fe[II] and Fe[III] can directly facilitate DA quinone production *via* their ability to form *d*-orbital bridges between DA and  $O_2$  (Miller *et al.* 1990) in multiple reactions with DA (Sun *et al.* 2018b).

L-DOPA is also capable of directly binding Fe; gastrointestinal absorption studies found that increasing pH reduced L-DOPA absorption due to the formation of a highly-stable Fe[III]:L-DOPA complex with 1:3 stoichiometry (Campbell *et al.* 1990, Zaidi & Fatima 2014). Within stressed neurons, acidosis from mitochondrial dysfunction keeps cytosolic pH slightly acidic (Balut *et al.* 2007), which favours the more stable Fe[II] and the oxidation-prone  $[Fe(OH)_2]^0$  complex at  $pH > 5$  (Morgan & Lahav 2007) and promotes oxidative stress in astrocyte-neuron co-cultures (Ying *et al.* 1999). Assuming the intracellular pH of a DAergic neuron is slightly acidic owing to acid loading typical of metabolically-active cells (Ruffin *et al.* 2014) – the pH of *post mortem* Parkinson's disease and age-matched control brain tissue has been reported as  $6.43 \pm 0.56$  and  $6.36 \pm 0.60$ , respectively (Genoud *et al.* 2017) – it is plausible

that L-DOPA is capable of chelating Fe[II] and preventing it reacting with cytosolic DA released from permeable vesicles. While L-DOPA can independently form neurotoxic L-dopaquinone (which in turn is a constituent of NM) by way of a short-lived Fe[III] intermediary, kinetics dictate that the reaction only goes to completion at very low pH, and even in conditions reflective of severe acidosis of pH <6.4 observed rate constants favour formation of the Fe[III]:L-DOPA complex (Linert *et al.* 1991).

Our findings showed no evidence L-DOPA potentiated neurotoxicity in either individual or the ‘two-hit’ combined Fe-overload and hA53T overexpression mouse models of parkinsonian neurodegeneration. Instead, we found evidence that L-DOPA may be partially neuroprotective, with the chronic treatment groups all showing normalised levels of midbrain Fe, including a dramatic reduction in SNc Fe concentration, decreased levels of protein carbonyls, and prevention of neurodegeneration in individual Fe-overload or hA53T transgenic models. As the hA53T  $\alpha$ -syn mutant has a known sensitivity to Fe (Zhu *et al.* 2016), the likely route of this protective effect involves the formation of stable Fe:L-DOPA complexes.

The total Fe complement of a neuron is within the  $\mu$ M range (Fiedler *et al.* 2007). It is estimated that the reactive labile iron pool (LIP) represents <5% of total cellular Fe in a redox-active and chelatable state (Kakhlon & Cabantchik 2002). With such high affinity to Fe, it is plausible that both CQ and L-DOPA are capable of forming stable complexes in the event of a pathological increase in the neuronal LIP. *In vitro* measurement of Fe:L-DOPA affinity found ferrous and ferric species form very stable 1:3 complexes (Fe[II]:L-DOPA  $K_{stab} = \sim 10^8$ ,  $pK_{stab} = -9$ ; Fe[III]:L-DOPA  $K_{stab} = \sim 10^{18}$ ,  $pK_{stab} = -3$ ) at pH 6.8-7.2 (Rajan *et al.* 1978). To our knowledge, the  $K_{stab}$  for our ‘control’ Fe-chelator CQ has not been reported, though 8-HQ, which binds Fe[II]/[III] *via* N and O electron donor sites with the same 1:3 stoichiometry (Prachayasittikul *et al.* 2013) forms even more stable complexes (Fe[II]:8-HQ  $K_{stab} = \sim 10^{15}$ ; Fe[III]:8-HQ  $K_{stab} = \sim 10^{36}$ ; (Zhou *et al.* 2012)) in a similar manner to deferiprone (DFP) (Devos *et al.* 2014), another high affinity Fe chelator (Fe[III]:CQ  $K_{stab} = \sim 10^{35}$ ) that is currently in Phase II trials for Parkinson’s disease (ClinicalTrials.gov Identifier: NCT02728843). At concentrations similar to our H<sub>2</sub>O<sub>2</sub> assay (50  $\mu$ M CQ, 20  $\mu$ M Fe<sup>2+</sup>) CQ chelates 91.2% of available Fe (Zheng *et al.* 2010).

Untreated A53T mice show no observable increases in total Fe levels at 8 months of age compared to WT, suggesting impaired DA trafficking or the single-point mutation does not itself trigger pathological Fe accumulation. While this  $\alpha$ -syn mutant has provided valuable information about synucleinopathy in movement disorders, no one genetic risk factor captures the multifaceted nature of idiopathic Parkinson's disease. For the purposes of this study, where the hA53T mutation induces the formation of vesicular membrane-permeabilising  $\alpha$ -syn protofibrils (Volles & Lansbury 2002) and is directly associated increased cytosolic DA levels (Lotharius & Brundin 2002a), the biochemical phenotype of disrupted DA metabolism and neurodegeneration is still suitable in the absence of Parkinson's disease-like Lewy pathology (Gispert *et al.* 2003). When challenged with excess Fe during a critical window of neurodevelopment, hA53T mice showed the expected increase in nigral Fe. Interestingly, excess Fe did not worsen or accelerate neuropathology; DAergic neuron loss was not exacerbated and levels of oxidative protein modifications did not differ from the control hA53T group.

The 5'-untranslated region of  $\alpha$ -syn mRNA does contain a predicted iron-responsive element based on H-ferritin sequencing (Friedlich *et al.* 2007), though there is no compelling evidence the protein promotes Fe-accumulation in Parkinson's disease. The protein can act as a ferrireductase, though no common mutation, including hA53T, alters the rate of Fe[III] reduction (Davies *et al.* 2011). Increased  $\alpha$ -syn expression in Parkinson's disease (Chiba-Falek *et al.* 2006) may instead be a response to elevated neuronal Fe, and we confirmed our previous report (Billings *et al.* 2016) that hA53T overexpressing mice do not abnormally accumulate Fe in the midbrain. Chemical interactions between  $\alpha$ -syn and Fe are generally characterised as a potential underlying cause of  $\alpha$ -syn aggregation (Lingor *et al.* 2017), though, as expected, we observed no Lewy pathology in Fe-loaded hA53T midbrain. In our case, regardless of whether excess nigral Fe is present with mutated hA53T  $\alpha$ -syn, we do not witness exacerbated neuronal loss and increased oxidation protein modification. Similar to our findings, Fe exposure in *Drosophila melanogaster* did not induced DA neurodegeneration when hA53T mutant was present (Bonilla-Ramirez *et al.* 2011). A recent study in N27 neuronal cells transfected with hA53T  $\alpha$ -syn and challenged with Fe showed a reduction in lipid peroxidation and reactive oxygen species (ROS) compared to Fe-insulted non-transfected cells (Sanchez Campos *et al.* 2018).

Clearly, the biochemical and motor deficits elicited by Fe-exposure during early life are more severe in hA53T mice. Neither L-DOPA nor CQ were able to abrogate oxidative damage and neuron loss as they could in WT mice, providing more supporting evidence that Fe-mediated DA oxidation by way of  $\alpha$ -syn dysfunction is an early pathochemical feature of parkinsonian neurodegeneration. A similar combined Fe accumulation and hA53T model, in this case where elevated dietary Fe was introduced to sexually-mature adult mice from two to four months of age, recapitulated several key preclinical symptoms that indicate Fe-DA toxicity is an early-stage event, including impaired gut motility and hyperactive motor coordination (Jia et al. 2018). This recent study independently verifies how acute dietary Fe exposure during a critical window of vulnerability (P10-P17) predisposes elevated midbrain (and specifically SNc) Fe levels with age, compared to chronic dietary Fe overexposure for three months in mature animals. This suggests that the Fe requirements during this seven-day period of neurodevelopment is substantially greater than the rate of dietary Fe uptake by the adult rodent brain (Chen *et al.* 2012) and has a larger impact on influx/efflux imbalance favouring brain Fe retention with age (Chen *et al.* 2014). Importantly, Jia et al. (2018) found that Fe-exposure during adulthood evoked a phenotype reflective of gastrointestinal disturbances in prodromal Parkinson's disease (Goldman & Postuma 2014) in both WT and hA53T mice, and overt neurodegeneration and striatal DA loss occurred only in 12-month-old Fe-exposed mutant  $\alpha$ -syn animals.

A limitation of this study is that there is no perfect animal model of Parkinson's disease, and the neurochemical environment of human DA neurons likely has nuanced differences from those within the murine brain. It is debated as to whether ageing rodent DA neurons produce NM (Kim *et al.* 2006, Dauer & Przedborski 2003, Sukhorukova *et al.* 2014), and if so it would be at lower levels than those seen in higher-order species (Fedorow *et al.* 2005). This is still a remarkably small amount: assuming NM deposition is a cumulative process resulting from a lifetime of DA metabolism, the aged human SNc yields only 5 mg g<sup>-1</sup> (wet tissue weight) of the NM (Aime *et al.* 2000). Neuromelanin synthesis is promoted by cytosolic DA levels, and inhibited with Fe chelators (Sulzer *et al.* 2000), and produces several neurotoxic quinones (Hare & Double 2016); and if this pathway is relatively minor in the rodent brain a key mechanism involved in human DAergic neuron loss cannot be appropriately modelled. However, it should also be acknowledged that NM in the human brain has a moderate Fe-binding capacity (Bohic et al. 2008, Double *et al.* 2008) with two specific sites with affinity to Fe[III] ( $K_{stab} = 10^{7-8}$ ; Double *et al.* (2003)). Whether NM can buffer excess Fe, or

conversely provide a source for the LIP if it becomes saturated, has not yet been established. As a direct component of the hypothesised pathogenic reaction causing oxidative stress in DAergic neurons, DA levels themselves play a major role in possible neurotoxicity. This was highlighted in a recent study that assessed DA-derived oxidative damage, lysosomal dysfunction and  $\alpha$ -syn oligomerisation in induced pluripotent stem cell-derived DA neurons from human and murine fibroblasts, including with confirmed single point mutations to *SNCA*. Across all measures, mouse-derived neuron contained negligible levels of oxidised DA and substantially lower measures of cell dysfunction compared to human neurons (Burbulla *et al.* 2017), again emphasising how chemical differences between species can result in an incomplete picture of the human condition.

In summary, the data presented here suggests that L-DOPA is able to mitigate oxidative damage from excessive midbrain Fe to a degree similar to CQ. This effect was somewhat muted in hA53T expressing mice, which are more susceptible to oxidative damage from Fe exposure (Peng *et al.* 2010). Importantly, we show that L-DOPA not potentiate oxidation of DA *in vivo*, in contrast to previous cell culture studies (Basma *et al.* 1995, Pardo *et al.* 1995).

#### **Acknowledgements and conflict of interest disclosure**

We wish to thank Professor Virginia Lee for providing the original hA53T mouse line from which animals in this report were descendants. We also wish to thank Ms Milawaty Nurjono for assistance with animal culling. The Florey Institute of Neuroscience and Mental Health acknowledge the strong support from the Victorian Government and in particular the funding from the Operational Infrastructure Support Grant. P.A.D and D.J.H. are supported by funds from the Australian Research Council Linkage Project scheme in partnership with Agilent Technologies and ESI Ltd (LP120200081). P.A.A. received a Future Fellowship from the Australian Research Council (FT120100030). The National Health and Medical Research Council supported this work with funds to S.L.G. (Career Development Fellowship 1085483), A.I.B. (Program Grant 1132604; Research Fellowship 1103703), P.A.A. (Project Grant 1025774), D.I.F. (Project Grants 1061761, 1044542, 1043992 and 509286) and D.J.H. (Career Development Fellowship in partnership with Agilent Technologies 1122981). D.I.F. also receives support from the Michael J. Fox Foundation for Parkinson's Research.

P.A.A. and D.I.F. are paid consultants to and shareholders in Prana Biotechnology Ltd. A.I.B. is a shareholder in Prana Biotechnology Ltd., Mesoblast Pty Ltd., Cogstate Pty Ltd., NextVet Ltd., Collaborative Medicinal Development Pty Ltd., and a paid consultant for Collaborative Medicinal Development Pty Ltd. P.A.D. and D.J.H. receive material and research support from Agilent Technologies and ESI Ltd.

## Supporting information

Additional Supporting Information may be found online in the supporting information tab for this article:

**Figure S1.** PCR confirmation of hA53T  $\alpha$ -syn expression in in-house bred <sup>+/+</sup>hA53T expressing mice.

**Figure S2.** Bodyweights at 3 months of age.

**Figure S3.** Mean and daily CQ intake.

**Figure S4.** Calibration curve and linear regression analysis for determining H<sub>2</sub>O<sub>2</sub> concentration.

**Figure S5.** Fe concentrations in cortex and cerebellum.

## Figure Legends:

**Fig. 1:** Metabolic pathway of DA degradation and NM biosynthesis. Enzymes with a redox-active iron centre and/or conversion by iron-mediated catalysis are marked in red, while COMT is marked in dark blue to denote a suspected role in enzymatic activity. The majority of DA is excreted from the CNS as either epinephrine or homovanillic acid, with a minor proportion oxidising to neurotoxic DA quinones (blue), several of which are tautomeric and cyclise to the 5,6-dihydroxyindoles and 5,6-indolequinone monomers that constitute the neuromelanin biopolymer. Insets: structures of CQ and DOPA decarboxylase inhibitor benserazide; and tris-L-DOPA:Fe complex. Abbreviations: AAAH, aromatic amino acid hydroxylases; AADH, aromatic amine dehydrogenase; AADC, aromatic L-amino acid decarboxylase; ALDH, aldehyde dehydrogenase; COMT, catechol-O-methyltransferase; CYP2D6, cytochrome P450 2D6; DBH, dopamine  $\beta$ -hydroxylase; DOPAC, 3,4-dihydroxyphenylacetic acid; DOPAL, 3,4-dihydroxyphenylacetaldehyde; MAO, monoamine oxidases; PNMT, phenylethanolamine N-methyltransferase.

**Fig. 2:** Pictorial representation of experimental design. Elements of this figure are reproduced from the Allen Institute for Brain Science's Brain Explorer 2 application (Lein *et al.* 2007).

**Fig. 3:** CQ and L-DOPA inhibits Fe-mediated production of H<sub>2</sub>O<sub>2</sub>. \*\*\*  $p < 0.001$ , one way ANOVA with Fisher's LSD *post hoc* test.  $n = 3$  replicates per group.

**Fig. 4:** Fe concentration in (a) midbrain (MB) and (b) CPu of Fe-loaded and CQ/L-DOPA-treated mice. \*\*/\*\*\*  $p < 0.05/0.01$  vs vehicle; #/###/####  $p < 0.05/0.01/0.001$  vs Fe-exposed; one way ANOVA with Fisher's LSD *post hoc* test.  $n = 4-6$  animals per group.

**Fig. 5:** Representative photomicrographs, LA-ICP-MS Fe maps and overlaid parallel sections. Sections stained for TH (left column) were used to identify the corresponding SNc (black arrow; VTA, white arrow; SNr, grey arrow; scale bar = 500  $\mu\text{m}$ ) on the serial section imaged using LA-ICP-MS (middle column) and are shown here overlaid (right column). LA-ICP-MS images are presented on the same colour scale representing a concentration range of 0 to  $>30 \mu\text{g g}^{-1}$ . The mean Fe concentration in the SN from (a) vehicle ( $\dagger$  removed outlier;  $n = 7$ ) (b) Fe-fed ( $n = 4$ ) and (c) Fe-fed and L-DOPA treated ( $n = 4$ ) showed (d) a specific elevation in Fe-fed animals (\* vs vehicle,  $p < 0.05$ ; one way ANOVA with Fisher's LSD *post hoc* test), which was significantly decreased by chronic L-DOPA treatment (### vs Fe-fed,  $p < 0.001$ ).

**Fig. 6:** Protein carbonyls in the mouse midbrain. (a) Representative dot blots from the WT experimental groups. (b) Protein carbonyls were increased in Fe-fed animals (\*\*\* vs vehicle;  $p < 0.001$ ; one way ANOVA with Fisher's LSD *post hoc* test;  $\dagger$  removed outlier). Compared to Fe-fed animals, protein carbonyls remained at baseline for all other treatment groups (### vs Fe-fed,  $p < 0.001$ ). (c) In hA53T mice levels of protein carbonyls showed high variance, limiting usefulness of statistical analysis. Protein carbonyls were paradoxically decreased in Fe-fed animals (\* vs vehicle,  $p < 0.05$ ), though it should be noted that protein carbonyl levels in all hA53T animals was around half of those observed in WT animals, suggesting a genotype effect.  $n = 4-6$  per group.

**Fig. 7:** Representative photomicrographs of coronal sections passing through the SNc (white arrow, top left panel) were used to assess cell loss in (a) WT and (b) hA53T mice. Scale bar = 500  $\mu$ m.

**Fig. 8:** (a) Total neuron numbers were decreased in WT, Fe-fed animals (\*\*\* vs vehicle;  $p < 0.001$ ; one way ANOVA with Fisher's LSD *post hoc* test), with L-DOPA and CQ treatment apparently preventing neuron loss (### vs Fe-fed;  $p < 0.001$ ). (b) Neuron loss from combined Fe-overload and hA53T expression could only be prevented using concomitant L-DOPA and CQ administration. (# vs Fe-fed;  $p < 0.05$ ). (c) The specificity of DAergic neuron loss was confirmed when neuron numbers were stratified according to TH-positive and TH-negative cells. hA53T mice showed varying responses to both Fe-loading and subsequent treatment with L-DOPA and CQ (\* vs vehicle;  $p < 0.05$ ; †, †† and ††† vs indicated comparison;  $p < 0.05, 0.01$  and  $0.001$ , respectively).  $n = 4-5$  animals per group.

**Fig. 9:** Time-to-turn (T-turn) and time to complete task (T-total) for pole testing of (a) WT and (b) hA53T mice. Statistically significant effects were only observed at 5 months, and only in WT animals (\*\*\* vs vehicle;  $p < 0.001$ ; one way ANOVA with Fisher's LSD *post hoc* test; #, ##, ### vs Fe-fed;  $p < 0.05, 0.01$  and  $0.001$ ).  $n = 4-6$  animals per group.

## References:

(2008) Guidelines to promote the wellbeing of animals used for scientific purposes. National Health and Medical Research Council, Canberra.

Aime, S., Bergamasco, B., Casu, M. et al. (2000) Isolation and  $^{13}\text{C}$ -NMR characterization of an insoluble proteinaceous fraction from substantia nigra of patients with parkinson's disease. *Mov. Disord.*, **15**, 977-981.

Alberico, S. L., Cassell, M. D. and Narayanan, N. S. (2015) The vulnerable ventral tegmental area in Parkinson's disease. *Basal Ganglia*, **5**, 51-55.

Asanuma, M., Miyazaki, I. and Ogawa, N. (2003) Dopamine- or L-DOPA-induced neurotoxicity: The role of dopamine quinone formation and tyrosinase in a model of Parkinson's disease. *Neurotox. Res.*, **5**, 165-176.

- Ashley, C. and Dunleavy, A. (2017) *The Renal Drug Handbook: The Ultimate Prescribing Guide for Renal Practitioners, 4th Edition*. CRC Press.
- Ayton, S. and Lei, P. (2014) Nigral iron elevation is an invariable feature of Parkinson's disease and is a sufficient cause of neurodegeneration. *BioMed Res. Int.*, **2014**, a581256.
- Balut, C., vandeVen, M., Despa, S., Lambrechts, I., Ameloot, M., Steels, P. and Smets, I. (2007) Measurement of cytosolic and mitochondrial pH in living cells during reversible metabolic inhibition. *Kidney Int.*, **73**, 226-232.
- Baquet, Z. C., Williams, D., Brody, J. and Smeyne, R. J. (2009) A comparison of model-based (2D) and design-based (3D) stereological methods for estimating cell number in the substantia nigra pars compacta (SNpc) of the C57BL/6J mouse. *Neuroscience*, **161**, 1082-1090.
- Bareggi, S. R. and Cornelli, U. (2012) Clioquinol: Review of its Mechanisms of Action and Clinical Uses in Neurodegenerative Disorders. *CNS Neurosci. Ther.*, **18**, 41-46.
- Barnham, K. J. and Bush, A. I. (2014) Biological metals and metal-targeting compounds in major neurodegenerative diseases. *Chem. Soc. Rev.*, **43**, 6727-6749.
- Basma, A. N., Morris, E. J., Nicklas, W. J. and Geller, H. M. (1995) L-DOPA Cytotoxicity to PC12 Cells in Culture Is via Its Autoxidation. *J. Neurochem.*, **64**, 825-832.
- Bates, C. A. and Zheng, W. (2014) Brain disposition of  $\alpha$ -Synuclein: roles of brain barrier systems and implications for Parkinson's disease. *Fluids and Barriers of the CNS*, **11**, 17.
- Berg, D., Postuma, R. B., Adler, C. H. et al. (2015) MDS research criteria for prodromal Parkinson's disease. *Mov. Disord.*, **30**, 1600-1611.
- Billings, J. L., Hare, D. J., Nurjono, M., Volitakis, I., Cherny, R. A. A., Bush, A. I., Adlard, P. A. and Finkelstein, D. I. (2016) Effects of Neonatal Iron Feeding and Chronic Clioquinol Administration on the Parkinsonian Human A53T Transgenic Mouse. *ACS Chem. Neurosci.*, **7**, 360-366.

- Biosa, A., Sandrelli, F., Beltramini, M., Greggio, E., Bubacco, L. and Bisaglia, M. (2017) Recent findings on the physiological function of DJ-1: Beyond Parkinson's disease. *Neurobiol. Dis.*, **108**, 65-72.
- Birkmayer, W. and Hornykiewicz, O. (1961) Der L-dioxyphenylalanin-effekt bei der Parkinson-akinese. *Wein Klin Wschr*, **73**, 787-788.
- Birkmayer, W. and Hornykiewicz, O. (1962) Der L-Dioxyphenylalanin-Effekt beim Parkinson-Syndrom des Menschen: zur Pathogenese und Behandlung der Parkinson-Akinese. *Arch. Psychiatr. Nervenkr.*, **203**, 560-574.
- Bohic, S., Murphy, K., Paulus, W., Cloetens, P., Salomé, M., Susini, J. and Double, K. (2008) Intracellular Chemical Imaging of the Developmental Phases of Human Neuromelanin Using Synchrotron X-ray Microspectroscopy. *Anal. Chem.*, **80**, 9557-9566.
- Bonilla-Ramirez, L., Jimenez-Del-Rio, M. and Velez-Pardo, C. (2011) Acute and chronic metal exposure impairs locomotion activity in *Drosophila melanogaster*: a model to study Parkinsonism. *BioMetals*, **24**, 1045-1057.
- Burbulla, L. F., Song, P., Mazzulli, J. R. et al. (2017) Dopamine oxidation mediates mitochondrial and lysosomal dysfunction in Parkinson's disease. *Science*, **357**, 1255-1261.
- Campbell, N. R. and Hasinoff, B. (1989) Ferrous sulfate reduces levodopa bioavailability: chelation as a possible mechanism. *Clin. Pharmacol. Ther.*, **45**, 220-225.
- Campbell, R. R. A., Hasinoff, B., Chernenko, G., Barrowman, J. and Campbell, N. R. C. (1990) The effect of ferrous sulfate and pH on L-dopa absorption. *Can. J. Physiol. Pharmacol.*, **68**, 603-607.
- Carvey, P. M., Zhao, C. H., Hendey, B., Lum, H., Trachtenberg, J., Desai, B. S., Snyder, J., Zhu, Y. G. and Ling, Z. D. (2005) 6-Hydroxydopamine- induced alterations in blood-brain barrier permeability. *Eur. J. Neurosci.*, **22**, 1158-1168.

- Chen, J.-H., Shahnava, S., Singh, N., Ong, W.-Y. and Walczyk, T. (2012) Stable iron isotope tracing reveals significant brain iron uptake in adult rats. *Metallomics*, **5**, 167-173.
- Chen, J.-H., Singh, N., Tay, H. and Walczyk, T. (2014) Imbalance of iron influx and efflux causes brain iron accumulation over time in the healthy adult rat. *Metallomics*, **6**, 1417-1426.
- Cherny, R. A., Atwood, C. S., Xilinas, M. E. et al. (2001) Treatment with a Copper-Zinc Chelator Markedly and Rapidly Inhibits  $\beta$ -Amyloid Accumulation in Alzheimer's Disease Transgenic Mice. *Neuron*, **30**, 665-676.
- Chesselet, M.-F. (2007) In vivo alpha-synuclein overexpression in rodents: A useful model of Parkinson's disease? *Exp. Neurol.*, **209**, 22-27.
- Chiba-Falek, O., Lopez, G. J. and Nussbaum, R. L. (2006) Levels of alpha-synuclein mRNA in sporadic Parkinson disease patients. *Mov. Disord.*, **21**, 1703-1708.
- Cotzias, G. C., Woert, M. H. and Schiffer, L. M. (1967) Aromatic Amino Acids and Modification of Parkinsonism. *N. Engl. J. Med.*, **276**, 374-379.
- Dalle-Donne, I., Rossi, R., Giustarini, D., Milzani, A. and Colombo, R. (2003) Protein carbonyl groups as biomarkers of oxidative stress. *Clin. Chim. Acta*, **329**, 23-38.
- Daubner, C. S., Le, T. and Wang, S. (2011) Tyrosine hydroxylase and regulation of dopamine synthesis. *Arch. Biochem. Biophys.*, **508**, 1-12.
- Dauer, W. and Przedborski, S. (2003) Parkinson's Disease Mechanisms and Models. *Neuron*, **39**, 889-909.
- Davies, P., Moualla, D. and Brown, D. R. (2011) Alpha-Synuclein Is a Cellular Ferrireductase. *PloS one*, **6**.
- de Silva, M. A., Mattern, C., Häcker, R., Tomaz, C., Huston, J. P. and Schwarting, R. K. W. (1997) Increased neostriatal dopamine activity after intraperitoneal or intranasal administration of L-DOPA: On the role of benserazide pretreatment. *Synapse*, **27**, 294-302.

- Devos, D., Moreau, C., Devedjian, J. et al. (2014) Targeting Chelatable Iron as a Therapeutic Modality in Parkinson's Disease. *Antiox. Redox. Signal.*, **21**, 195-210.
- Di Monte, D. A. (2003) The environment and Parkinson's disease: is the nigrostriatal system preferentially targeted by neurotoxins? *The Lancet Neurology*, **2**, 531-538.
- Dixon, S. J. and Stockwell, B. R. (2014) The role of iron and reactive oxygen species in cell death. *Nat. Chem. Biol.*, **10**, 9-17.
- Double, K. L., Dedov, V. N., Fedorow, H., Kettle, E., Halliday, G. M., Garner, B. and Brunk, U. T. (2008) The comparative biology of neuromelanin and lipofuscin in the human brain. *Cell. Mol. Life Sci.*, **65**, 1669-1682.
- Double, K. L., Gerlach, M., Schünemann, V., Trautwein, A. X., Zecca, L., Gallorini, M., Youdim, M., Riederer, P. and Ben-Shachar, D. (2003) Iron-binding characteristics of neuromelanin of the human substantia nigra. *Biochem. Pharmacol.*, **66**, 489-494.
- Fahn, S., Oakes, D., Shoulson, I. et al. (2004) Levodopa and the progression of Parkinson's disease. *N. Engl. J. Med.*, **351**, 2498-2508.
- Fedorow, H., Tribl, F., Halliday, G., Gerlach, M., Riederer, P. and Double, K. L. (2005) Neuromelanin in human dopamine neurons: Comparison with peripheral melanins and relevance to Parkinson's disease. *Prog. Neurobiol.*, **75**, 109-124.
- Fiedler, A., Reinert, T., Morawski, M., Brückner, G., Arendt, T. and Butz, T. (2007) Intracellular iron concentration of neurons with and without perineuronal nets. *Nucl. Instrum. Methods Phys. Res., Sect. B*, **260**, 153-158.
- Finkelstein, D., Hare, D., Billings, J. et al. (2016) Clioquinol Improves Cognitive, Motor Function, and Microanatomy of the Alpha-Synuclein hA53T Transgenic Mice. *ACS Chem. Neurosci.*, **7**.
- Finkelstein, D. I., Billings, J. L., Adlard, P. A. et al. (2017) The novel compound PBT434 prevents iron mediated neurodegeneration and alpha-synuclein toxicity in multiple models of Parkinson's disease. *Acta Neuropathol. Commun.*, **5**, 53.

- Finkelstein, D. I., Stanic, D., Parish, C. L., Tomas, D., Dickson, K. and Horne, M. K. (2000) Axonal sprouting following lesions of the rat substantia nigra. *Neuroscience*, **97**, 99-112.
- Fleming, S. M., Salcedo, J., Fernagut, P.-O., Rockenstein, E., Masliah, E., Levine, M. S. and Chesselet, M.-F. (2004) Early and Progressive Sensorimotor Anomalies in Mice Overexpressing Wild-Type Human  $\alpha$ -Synuclein. *The Journal of Neuroscience*, **24**, 9434-9440.
- Foster, H. D. and Hoffer, A. (2004) The two faces of L-DOPA: benefits and adverse side effects in the treatment of Encephalitis lethargica, Parkinson's disease, multiple sclerosis and amyotrophic lateral sclerosis. *Med. Hypotheses*, **62**, 177-181.
- Fredriksson, A., Schröder, N., Eriksson, P., Izquierdo, I. and Archer, T. (1999) Neonatal Iron Exposure Induces Neurobehavioural Dysfunctions in Adult Mice. *Toxicol. Appl. Pharmacol.*, **159**, 25-30.
- Fredriksson, A., Schröder, N., Eriksson, P., Izquierdo, I. and Archer, T. (2001) Neonatal iron potentiates adult MPTP-induced neurodegenerative and functional deficits. *Parkinsonism & Related Disorders*, **7**, 97-105.
- Friedlich, A. L., Tanzi, R. E. and Rogers, J. T. (2007) The 5'-untranslated region of Parkinson's disease  $\alpha$ -synuclein messengerRNA contains a predicted iron responsive element. *Mol. Psychiatry*, **12**, 222-223.
- Genoud, S., Roberts, B. R., Gunn, A. P., Halliday, G. M., Lewis, S. J. G., Ball, H. J., Hare, D. J. and Double, K. L. (2017) Subcellular compartmentalisation of copper, iron, manganese, and zinc in the Parkinson's disease brain. *Metallomics*, **9**, 1447-1455.
- Giasson, B. I., Duda, J. E., Quinn, S. M., Zhang, B., Trojanowski, J. Q. and Lee, V. (2002) Neuronal  $\alpha$ -Synucleinopathy with Severe Movement Disorder in Mice Expressing A53T Human  $\alpha$ -Synuclein. *Neuron*, **34**, 521-533.
- Gispert, S., Turco, D., Garrett, L. et al. (2003) Transgenic mice expressing mutant A53T human alpha-synuclein show neuronal dysfunction in the absence of aggregate formation. *Mol. Cell. Neurosci.*, **24**, 419-429.

- Goldman, J. G. and Postuma, R. (2014) Premotor and nonmotor features of Parkinson's disease. *Curr. Opin. Neurol.*, **27**, 434-441.
- Gordeuk, V. R., Brittenham, G. M., McLaren, C. E., Hughes, M. A. and Keating, L. J. (1986) Carbonyl iron therapy for iron deficiency anemia. *Blood*, **67**, 745-752.
- Gray, M. T. and Woulfe, J. M. (2015) Striatal Blood–Brain Barrier Permeability in Parkinson's Disease. *J. Cereb. Blood Flow Metab.*, **35**, 747-750.
- Gundersen, H. J. G., Bagger, P., Bendtsen, T. F. et al. (1988) The new stereological tools: Disector, fractionator, nucleator and point sampled intercepts and their use in pathological research and diagnosis. *Acta Pathologica, Microbiologica, et Immunologica Scandinavica*, **96**, 857-881.
- Hare, D., Reedy, B., Grimm, R. et al. (2009) Quantitative elemental bio-imaging of Mn, Fe, Cu and Zn in 6-hydroxydopamine induced Parkinsonism mouse models. *Metallomics*, **1**, 53-58.
- Hare, D. J., Adlard, P. A., Doble, P. A. and Finkelstein, D. I. (2013a) Metallobiology of 1-methyl-4-phenyl-1,2,3,6-tetrahydropyridine neurotoxicity. *Metallomics*, **5**, 91-109.
- Hare, D. J., Arora, M., Jenkins, N. L., Finkelstein, D. I., Doble, P. A. and Bush, A. I. (2015) Is early-life iron exposure critical in neurodegeneration? *Nat. Rev. Neurol.*, **11**, 536-544.
- Hare, D. J., Cardoso, B., Raven, E. P., Double, K. L., Finkelstein, D. I., Szymlek-Gay, E. A. and Biggs, B.-A. (2017a) Excessive early-life dietary exposure: a potential source of elevated brain iron and a risk factor for Parkinson's disease. *NPJ Parkinsons Dis.*, **3**, 1-5.
- Hare, D. J., Cardoso, B., Szymlek-Gay, E. A. and Biggs, B.-A. (2018) Neurological effects of iron supplementation in infancy: finding the balance between health and harm in iron-replete infants. *Lancet Child Adolesc. Health*, **2**, 144-156.
- Hare, D. J. and Double, K. L. (2016) Iron and dopamine: a toxic couple. *Brain*, **139**, 1026-1035.

- Hare, D. J., George, J. L., Bray, L. et al. (2013b) The effect of paraformaldehyde fixation and sucrose cryoprotection on metal concentration in murine neurological tissue. *J. Anal. At. Spectrom.*, **29**, 565-570.
- Hare, D. J., Kysenius, K., Paul, B. et al. (2017b) Imaging Metals in Brain Tissue by Laser Ablation - Inductively Coupled Plasma - Mass Spectrometry (LA-ICP-MS). *J. Vis. Exp.*, 55042.
- Hare, D. J., Lear, J., Bishop, D., Beavis, A. and Doble, P. A. (2013c) Protocol for production of matrix-matched brain tissue standards for imaging by laser ablation-inductively coupled plasma- mass spectrometry. *Anal. Methods*, **5**, 1915-1921.
- Hare, D. J., Lee, J. K., Beavis, A. D., van Gramberg, A., George, J., Adlard, P. A., Finkelstein, D. I. and Doble, P. A. (2012) Three-Dimensional Atlas of Iron, Copper, and Zinc in the Mouse Cerebrum and Brainstem. *Anal. Chem.*, **84**, 3990-3997.
- Hare, D. J., Lei, P., Ayton, S. et al. (2014) An iron–dopamine index predicts risk of parkinsonian neurodegeneration in the substantia nigra pars compacta. *Chem. Sci.*, **5**, 2160-2169.
- He, N., Ling, H., Ding, B., Huang, J., Zhang, Y., Zhang, Z., Liu, C., Chen, K. and Yan, F. (2015) Region-specific disturbed iron distribution in early idiopathic Parkinson's disease measured by quantitative susceptibility mapping. *Hum. Brain Mapp.*, **36**, 4407-4420.
- Hefti, F., Melamed, E., Bhawan, J. and Wurtman, R. J. (1981) Long-term administration of L-DOPA does not damage dopaminergic neurons in the mouse. *Neurology*, **31**, 1194-1195.
- Hely, M. A., Morris, J., Reid, W. and Trafficante, R. (2005) Sydney multicenter study of Parkinson's disease: Non-L- dopa –responsive problems dominate at 15 years. *Mov. Disord.*, **20**, 190-199.
- Herrera, A., Muñoz, P., Steinbusch, H. W. M. and Segura-Aguilar, J. (2017) Are Dopamine Oxidation Metabolites Involved in the Loss of Dopaminergic Neurons in the Nigrostriatal System in Parkinson's Disease? *ACS Chem. Neurosci.*, **8**, 702-711.

- James, S. A., Roberts, B. R., Hare, D. J., de Jonge, M. D., Birchall, I. E., Jenkins, N. L., Cherny, R. A., Bush, A. I. and McColl, G. (2015) Direct in vivo imaging of ferrous iron dyshomeostasis in ageing *Caenorhabditis elegans*. *Chem. Sci.*, **6**, 2952-2962.
- Jia, F., Song, N., Wang, W., Du, X., Chi, Y. and Jiang, H. (2018) High Dietary Iron Supplement Induces the Nigrostriatal Dopaminergic Neurons Lesion in Transgenic Mice Expressing Mutant A53T Human Alpha-Synuclein. *Front. Aging Neurosci.*, **10**, 97.
- Jiang, T., Sun, Q. and Chen, S. (2016) Oxidative stress: A major pathogenesis and potential therapeutic target of antioxidative agents in Parkinson's disease and Alzheimer's disease. *Prog. Neurobiol.*, **147**, 1-19.
- Jonkers, N., Sarre, S., Ebinger, G. and Michotte, Y. (2001) Benserazide decreases central AADC activity, extracellular dopamine levels and levodopa decarboxylation in striatum of the rat. *J. Neural. Transm.*, **108**, 559-570.
- Kakhlon, O. and Cabantchik, Z. I. (2002) The labile iron pool: characterization, measurement, and participation in cellular processes. *Free Radic. Biol. Med.*, **33**, 1037-1046.
- Kalia, L. V. and Lang, A. E. (2016) Parkinson disease in 2015: Evolving basic, pathological and clinical concepts in PD. *Nat. Rev. Neurol.*, **12**, 65-66.
- Katzenschlager, R., Head, J., Schrag, A., Ben-Shlomo, Y., Evans, A., Lees, A. J. and of the Kingdom, P. s. (2008) Fourteen-year final report of the randomized PDRG-UK trial comparing three initial treatments in PD. *Neurology*, **71**, 474-480.
- Kaur, D., Peng, J., Chinta, S. J., Rajagopalan, S., Monte, D. A., Cherny, R. A. and Andersen, J. K. (2007) Increased murine neonatal iron intake results in Parkinson-like neurodegeneration with age. *Neurobiol. Aging*, **28**, 907-913.
- Kaur, D., Yantiri, F., Rajagopalan, S. et al. (2003) Genetic or Pharmacological Iron Chelation Prevents MPTP-Induced Neurotoxicity In Vivo A Novel Therapy for Parkinson's Disease. *Neuron*, **37**, 899-909.

- Kim, S., Choi, J., Kim, D. and Hwang, O. (2006) Increases in TH immunoreactivity, neuromelanin and degeneration in the substantia nigra of middle aged mice. *Neurosci. Lett.*, **396**, 263-268.
- Kordower, J. H., Olanow, W. C., Dodiya, H. B., Chu, Y., Beach, T. G., Adler, C. H., Halliday, G. M. and Bartus, R. T. (2013) Disease duration and the integrity of the nigrostriatal system in Parkinson's disease. *Brain*, **136**, 2419-2431.
- Kulagina, N. V. and Michael, A. C. (2003) Monitoring Hydrogen Peroxide in the Extracellular Space of the Brain with Amperometric Microsensors. *Anal. Chem.*, **75**, 4875-4881.
- Lai, C.-T. and Yu, P. H. (1997) Dopamine-and L- $\beta$ -3, 4-dihydroxyphenylalanine hydrochloride (L-Dopa)-induced cytotoxicity towards catecholaminergic neuroblastoma SH-SY5Y cells: Effects of oxidative stress and antioxidative factors. *Biochem. Pharmacol.*, **53**, 363-372.
- Lang, A. E. and Espay, A. J. (2018) Disease Modification in Parkinson's Disease: Current Approaches, Challenges, and Future Considerations. *Mov. Disord.*, **33**, 660-677.
- Lear, J., Hare, D., Adlard, P., Finkelstein, D. and Doble, P. (2012a) Improving acquisition times of elemental bio-imaging for quadrupole-based LA-ICP-MS. *J. Anal. At. Spectrom.*, **27**, 159-164.
- Lear, J., Hare, D. J., Fryer, F., Adlard, P. A., Finkelstein, D. I. and Doble, P. A. (2012b) High-Resolution Elemental Bioimaging of Ca, Mn, Fe, Co, Cu, and Zn Employing LA-ICP-MS and Hydrogen Reaction Gas. *Anal. Chem.*, **84**, 6707-6714.
- Lee, P.-C., Raaschou-Nielsen, O., Lill, C. M., Bertram, L., Sinsheimer, J. S., Hansen, J. and Ritz, B. (2016) Gene-environment interactions linking air pollution and inflammation in Parkinson's disease. *Environ. Res.*, **151**, 713-720.
- Lein, E. S., Hawrylycz, M. J., Ao, N. et al. (2007) Genome-wide atlas of gene expression in the adult mouse brain. *Nature*, **445**.
- Li, C.-L., Werner, P. and Cohen, G. (1995) Lipid Peroxidation in Brain: Interactions of L-DOPA/Dopamine with Ascorbate and Iron. *Neurodegeneration*, **4**, 147-154.

- Linert, W., Jameson, R. F. and Herlinger, E. (1991) Complex formation followed by internal electron transfer: the reaction between L-dopa and iron(III). *Inorg. Chim. Acta*, **187**, 239-247.
- Lingor, P., Carboni, E. and Koch, J. (2017) Alpha-synuclein and iron: two keys unlocking Parkinson's disease. *J. Neural. Transm.*, DOI: 10.1007/s00702-00017-01695-x.
- Lipski, J., Nistico, R., Berretta, N., Guatteo, E., Bernardi, G. and Mercuri, N. B. (2011) L-DOPA: A scapegoat for accelerated neurodegeneration in Parkinson's disease? *Prog. Neurobiol.*, **94**, 389-407.
- Lotharius, J. and Brundin, P. (2002a) Impaired dopamine storage resulting from  $\alpha$ -synuclein mutations may contribute to the pathogenesis of Parkinson's disease. *Hum. Mol. Genet.*, **11**, 2395-2407.
- Lotharius, J. and Brundin, P. (2002b) Pathogenesis of parkinson's disease: dopamine, vesicles and  $\alpha$ -synuclein. *Nat. Rev. Neurosci.*, **3**, 932-942.
- Lu, H., Chen, J., Huang, H., Zhou, M., Zhu, Q., Yao, S. Q., Chai, Z. and Hu, Y. (2017) Iron modulates the activity of monoamine oxidase B in SH-SY5Y cells. *BioMetals*, **30**, 599-607.
- Matsuura, K., Kabuto, H., Makino, H. and Ogawa, N. (1997) Pole test is a useful method for evaluating the mouse movement disorder caused by striatal dopamine depletion. *J. Neurosci. Methods*, **73**, 45-48.
- Mercuri, N. and Bernardi, G. (2005) The 'magic' of l-dopa: why is it the gold standard Parkinson's disease therapy? *Trends Pharmacol. Sci.*, **26**, 341-344.
- Miller, D. M., Buettner, G. R. and Aust, S. D. (1990) Transition metals as catalysts of "autoxidation" reactions. *Free Radic. Biol. Med.*, **8**, 95-108.
- Morgan, B. and Lahav, O. (2007) The effect of pH on the kinetics of spontaneous Fe(II) oxidation by O<sub>2</sub> in aqueous solution – basic principles and a simple heuristic description. *Chemosphere*, **68**, 2080-2084.

- Moscovitz, O., Ben-Nissan, G., Fainer, I., Pollack, D., Mizrahi, L. and Sharon, M. (2015) The Parkinson's-associated protein DJ-1 regulates the 20S proteasome. *Nat. Commun.*, **6**, 6609.
- Olanow, W. C. (2015) Levodopa: Effect on cell death and the natural history of Parkinson's disease. *Mov. Disord.*, **30**, 37-44.
- Opazo, C., Huang, X., Cherny, R. A. et al. (2002) Metalloenzyme-like Activity of Alzheimer's Disease  $\beta$ -Amyloid Cu-Dependent Catalytic Conversion Of Dopamine, Cholesterol, And Biological Reducing Agents To Neurotoxic  $H_2O_2$ . *J. Biol. Chem.*, **277**, 40302-40308.
- Ostrerova-Golts, N., Petrucelli, L., Hardy, J., Lee, J. M., Farer, M. and Wolozin, B. (2000) The A53T alpha-synuclein mutation increases iron-dependent aggregation and toxicity. *J. Neurosci.*, **20**, 6048-6054.
- Papanikolaou, G. and Pantopoulos, K. (2005) Iron metabolism and toxicity. *Toxicol. Appl. Pharmacol.*, **202**, 199-211.
- Pardo, B., Mena, M. A., Casarejos, M. J., Paíno, C. L. and Yébenes, J. G. (1995) Toxic effects of L-DOPA on mesencephalic cell cultures: protection with antioxidants. *Brain Res.*, **682**, 133-143.
- Parish, C. L., Stanic, D., Drago, J., Borrelli, E., Finkelstein, D. I. and Horne, M. K. (2002) Effects of long-term treatment with dopamine receptor agonists and antagonists on terminal arbor size. *Eur. J. Neurosci.*, **16**, 787-794.
- Parkkinen, L., O'Sullivan, S. S., Kuoppamäki, M., Collins, C., Kallis, C., Holton, J. L., Williams, D. R., Revesz, T. and Lees, A. J. (2011) Does levodopa accelerate the pathologic process in Parkinson disease brain? *Neurology*, **77**, 1420-1426.
- Peng, J., Oo, M. and Andersen, J. K. (2010) Synergistic effects of environmental risk factors and gene mutations in Parkinson's disease accelerate age-related neurodegeneration. *J. Neurochem.*, **115**, 1363-1373.
- Pennington, K., Peng, J., Hung, C.-C., Banks, R. E. and Robinson, P. A. (2010) Differential effects of wild-type and A53T mutant isoform of alpha-synuclein on the

- mitochondrial proteome of differentiated SH-SY5Y cells. *J. Proteome Res.*, **9**, 2390-2401.
- Perry, T. L., Yong, V., Ito, M., Foulks, J. G., Wall, R. A., Godin, D. V. and Clavier, R. M. (1984) Nigrostriatal Dopaminergic Neurons Remain Undamaged in Rats Given High Doses of L-DOPA and Carbidopa Chronically. *J. Neurochem.*, **43**, 990-993.
- Prachayasittikul, V., Prachayasittikul, V., Prachayasittikul, S. and Ruchirawat, S. (2013) 8-Hydroxyquinolines: a review of their metal chelating properties and medicinal applications. *Drug Des. Devel. Ther.*, **7**, 1157-1178.
- Prada, D. M., Kettler, R., Zürcher, G., Schaffner, R. and Haefely, W. E. (1987) Inhibition of Decarboxylase and Levels of Dopa and 3-O-Methyldopa: A Comparative Study of Benserazide versus Carbidopa in Rodents and of Madopar Standard versus Madopar HBS in Volunteers. *Eur. Neurol.*, **27**, 9-20.
- Rajan, K. S., Mainer, S. and Davis, J. M. (1978) Studies on chelation of L-DOPA with metal ions and metal-ATP systems. *Bioinorg. Chem.*, **9**, 187-203.
- Ruffin, V. A., Salameh, A. I., Boron, W. F. and Parker, M. D. (2014) Intracellular pH regulation by acid-base transporters in mammalian neurons. *Frontiers in Physiology*, **5**, 43.
- Sanchez Campos, S., Alza, N. P. and Salvador, G. A. (2018) Lipid metabolism alterations in the neuronal response to A53T alpha-synuclein and Fe-induced injury. *Arch. Biochem. Biophys.*, **655**, 43-54.
- Segura-Aguilar, J., Paris, I., Muñoz, P., Ferrari, E., Zecca, L. and Zucca, F. A. (2014) Protective and toxic roles of dopamine in Parkinson's disease. *J. Neurochem.*, **129**, 898-915.
- Seibt, T. M., Proneth, B. and Conrad, M. (2018) Role of GPX4 in ferroptosis and its pharmacological implication. *Free Radic. Biol. Med.*
- Sian, J., Dexter, D. T., Lees, A. J., Daniel, S., Agid, Y., Javoy-Agid, F., Jenner, P. and Marsden, C. D. (1994) Alterations in glutathione levels in Parkinson's disease and other neurodegenerative disorders affecting basal ganglia. *Ann. Neurol.*, **36**, 348-355.

- Sobotka, T. J., Whittaker, P., Sobotka, J. M., Brodie, R. E., Wander, D. Y., Robl, M., Bryant, M. and Barton, C. N. (1996) Neurobehavioral dysfunctions associated with dietary iron overload. *Physiol. Behav.*, **59**, 213-219.
- Song, N. and Xie, J. (2018) Iron, Dopamine, and  $\alpha$ -Synuclein Interactions in at-Risk Dopaminergic Neurons in Parkinson's Disease. *Neurosci. Bull.*, **34**, 382-384.
- Sukhorukova, E. G., Alekseeva, O. S. and Korzhevsky, D. E. (2014) Catecholaminergic neurons of mammalian brain and neuromelanin. *Journal of Evolutionary Biochemistry and Physiology*, **50**, 383-391.
- Sulzer, D. (2007) Multiple hit hypotheses for dopamine neuron loss in Parkinson's disease. *Trends Neurosci.*, **30**, 244-250.
- Sulzer, D., Bogulavsky, J., Larsen, K. E. et al. (2000) Neuromelanin biosynthesis is driven by excess cytosolic catecholamines not accumulated by synaptic vesicles. *Proc. Natl. Acad. Sci. U. S. A.*, **97**, 11869-11874.
- Sun, Y., Pham, A. and Waite, D. T. (2018a) The effect of vitamin C and iron on dopamine-mediated free radical generation: implications to Parkinson's disease. *Dalton Trans.*, **47**, 4059-4069.
- Sun, Y., Pham, A. N., Hare, D. J. and Waite, T. D. (2018b) Kinetic modelling of pH-dependent oxidation of dopamine by iron and its relevance to Parkinson's disease. *Front. Neurosci.*, in press.
- Sun, Y., Pham, N. A. and Waite, D. T. (2016) Elucidation of the interplay between Fe(II), Fe(III), and dopamine with relevance to iron solubilization and reactive oxygen species generation by catecholamines. *J. Neurochem.*, **137**, 955-968.
- Surmeier, J. D., Obeso, J. A. and Halliday, G. M. (2017) Selective neuronal vulnerability in Parkinson disease. *Nat. Rev. Neurosci.*, **18**, 101-113.
- Trist, B., Davies, K., Cottam, V. et al. (2017) Amyotrophic lateral sclerosis-like superoxide dismutase 1 proteinopathy is associated with neuronal loss in Parkinson's disease brain. *Acta Neuropathol.*, **134**, 113-127.

- Tysnes, O.-B. and Storstein, A. (2017) Epidemiology of Parkinson's disease. *J. Neural. Transm.*, **124**, 901-905.
- Verschuur, C. V. M., Suwijn, S. R., Post, B. et al. (2015) Protocol of a randomised delayed-start double-blind placebo-controlled multi-centre trial for Levodopa in EARly Parkinson's disease: the LEAP-study. *BMC Neurol.*, **15**, 236.
- Vidgren, J. (1997) X-Ray Crystallography of Catechol O-Methyltransferase: Perspectives for Target-Based Drug Development. In: *Adv. Pharmacol.*, (D. S. Goldstein, G. Eisenhofer and R. McCarty eds.), Vol. 42, pp. 328-331. Academic Press.
- Volles, M. J. and Lansbury, P. T. (2002) Vesicle permeabilization by protofibrillar alpha-synuclein is sensitive to Parkinson's disease-linked mutations and occurs by a pore-like mechanism. *Biochemistry (Mosc.)*, **41**, 4595-4602.
- Waldmeier, P. C., Buchle, A.-M. and Steulet, A.-F. (1993) Inhibition of catechol-O-methyltransferase (COMT) as well as tyrosine and tryptophan hydroxylase by the orally active iron chelator, 1,2-dimethyl-3-hydroxypyridin-4-one (L1, CP20), in rat brain in vivo. *Biochem. Pharmacol.*, **45**, 2417-2424.
- Ward, R. J., Zucca, F. A., Duyn, J. H., Crichton, R. R. and Zecca, L. (2014) The role of iron in brain ageing and neurodegenerative disorders. *Lancet Neurol.*, **13**, 1045-1060.
- Weinstain, R., Savariar, E. N., Felsen, C. N. and Tsien, R. Y. (2014) In Vivo Targeting of Hydrogen Peroxide by Activatable Cell-Penetrating Peptides. *J. Am. Chem. Soc.*, **136**, 874-877.
- Ying, W., Han, S. K., Miller, J. W. and Swanson, R. A. (1999) Acidosis Potentiates Oxidative Neuronal Death by Multiple Mechanisms. *J. Neurochem.*, **73**, 1549-1556.
- Zaidi, S. Z. A. and Fatima, N. (2014) A comparative study for chelation of iron(II) and iron(III) with levodopa - an antiparkinsonian drug molecules. *European Chemical Bulletin*, **3**, 648-653.
- Zheng, H., Youdim, M. B. H. and Fridkin, M. (2010) Selective Acetylcholinesterase Inhibitor Activated by Acetylcholinesterase Releases an Active Chelator with Neurorescuing and Anti-Amyloid Activities. *ACS Chem. Neurosci.*, **1**, 737-746.

Zhou, T., Ma, Y., Kong, X. and Hider, R. C. (2012) Design of iron chelators with therapeutic application. *Dalton Trans.*, **41**, 6371-6389.

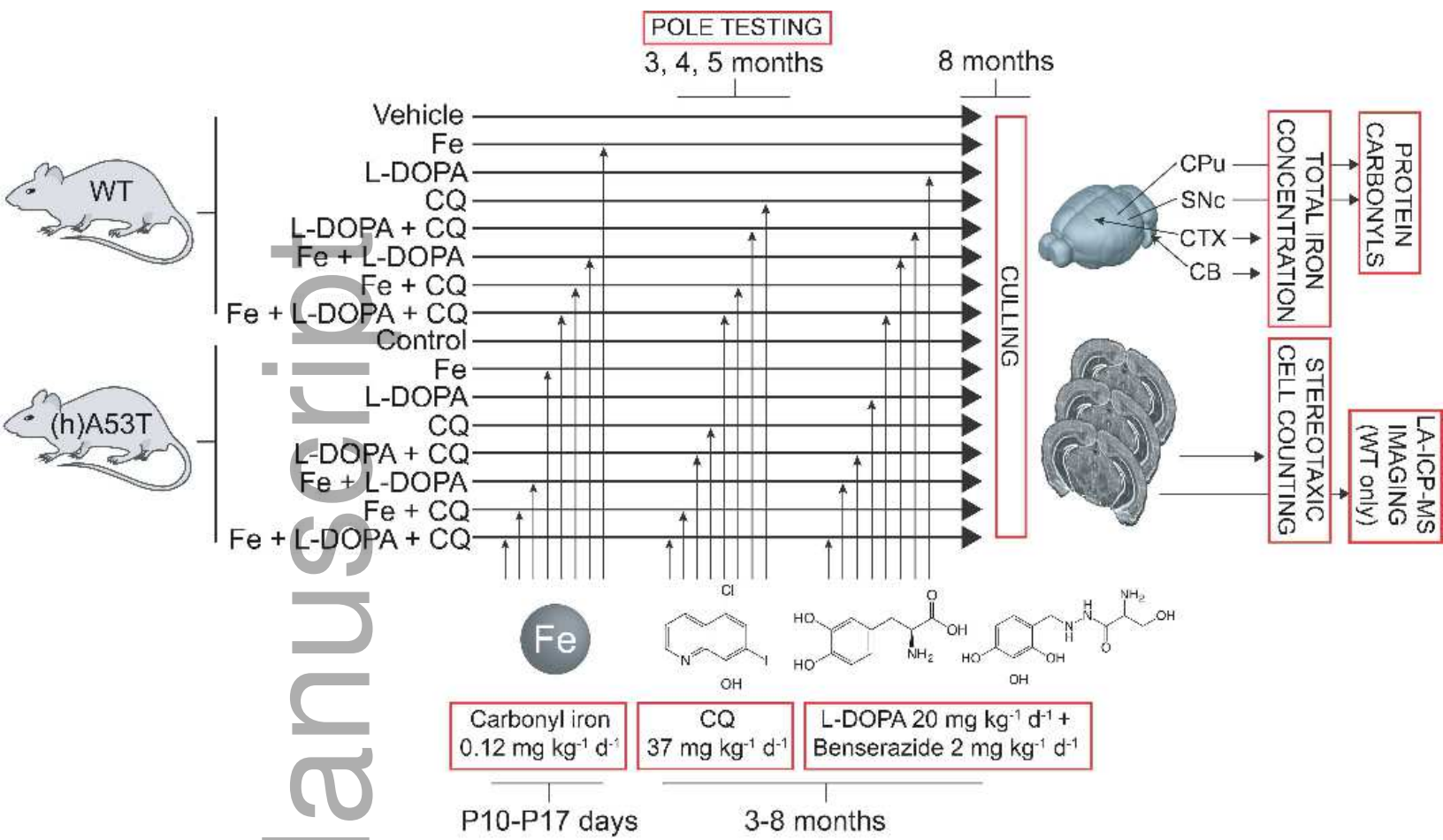
Zhu, Z.-J., Wu, K.-C., Yung, W.-H., Qian, Z.-M. and Ke, Y. (2016) Differential interaction between iron and mutant alpha-synuclein causes distinctive Parkinsonian phenotypes in *Drosophila*. *Biochim. Biophys. Acta, Mol. Basis Dis.*, **1862**, 518-525.

Zucca, F. A., Segura-Aguilar, J., Ferrari, E., Muñoz, P., Paris, I., Sulzer, D., Sarna, T., Casella, L. and Zecca, L. (2017) Interactions of iron, dopamine and neuromelanin pathways in brain aging and Parkinson's disease. *Prog. Neurobiol.*, **155**, 96-119.

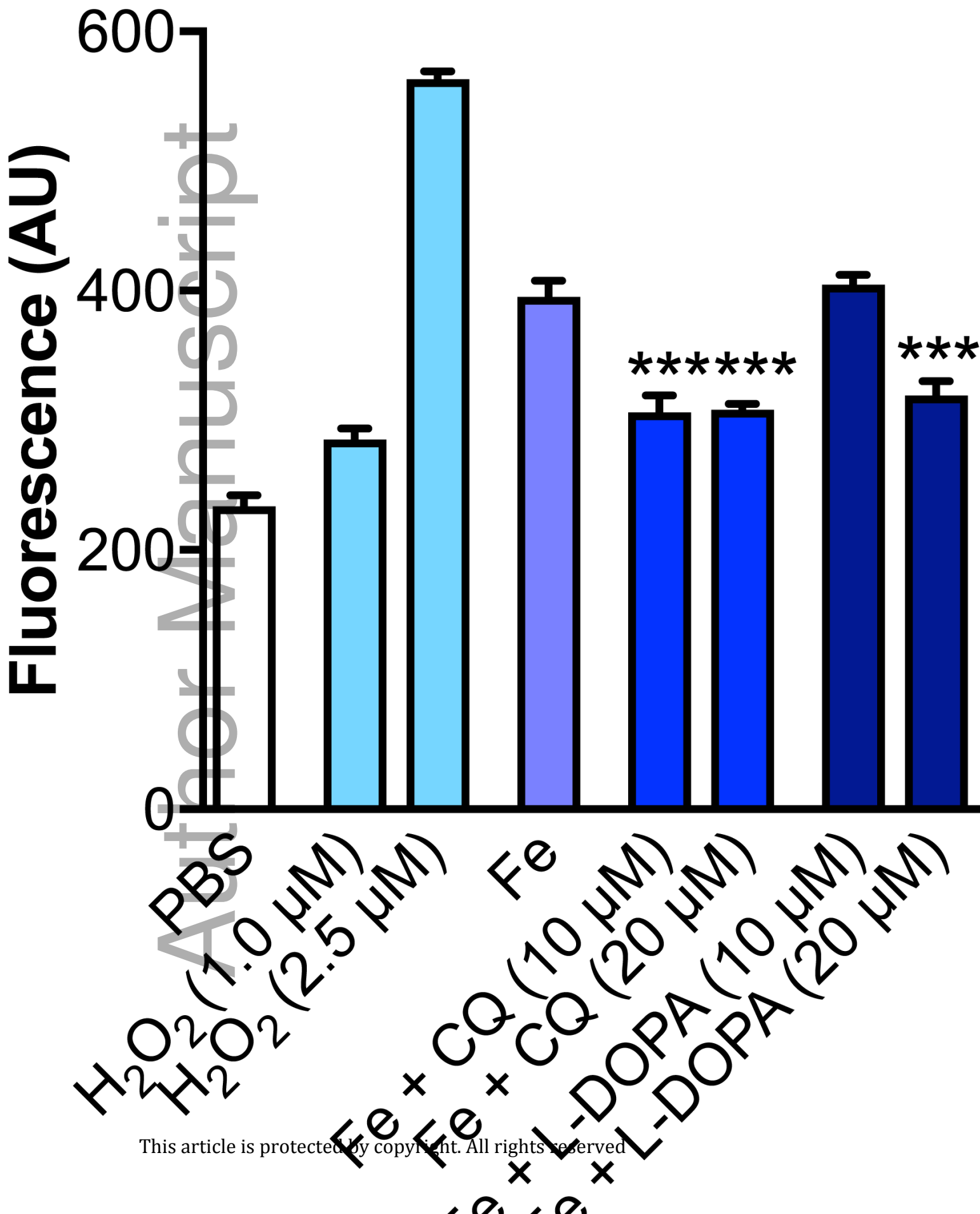
Author Manuscript

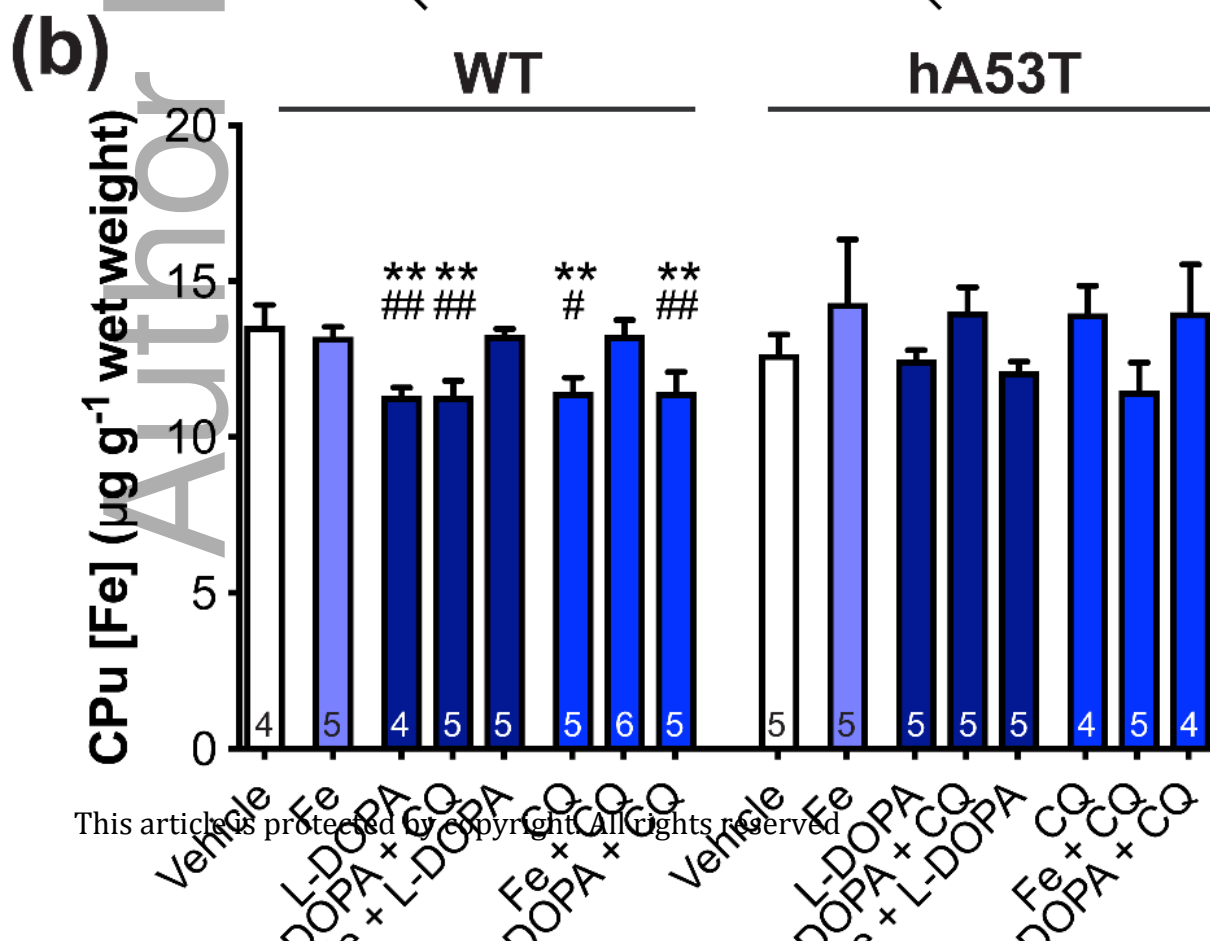
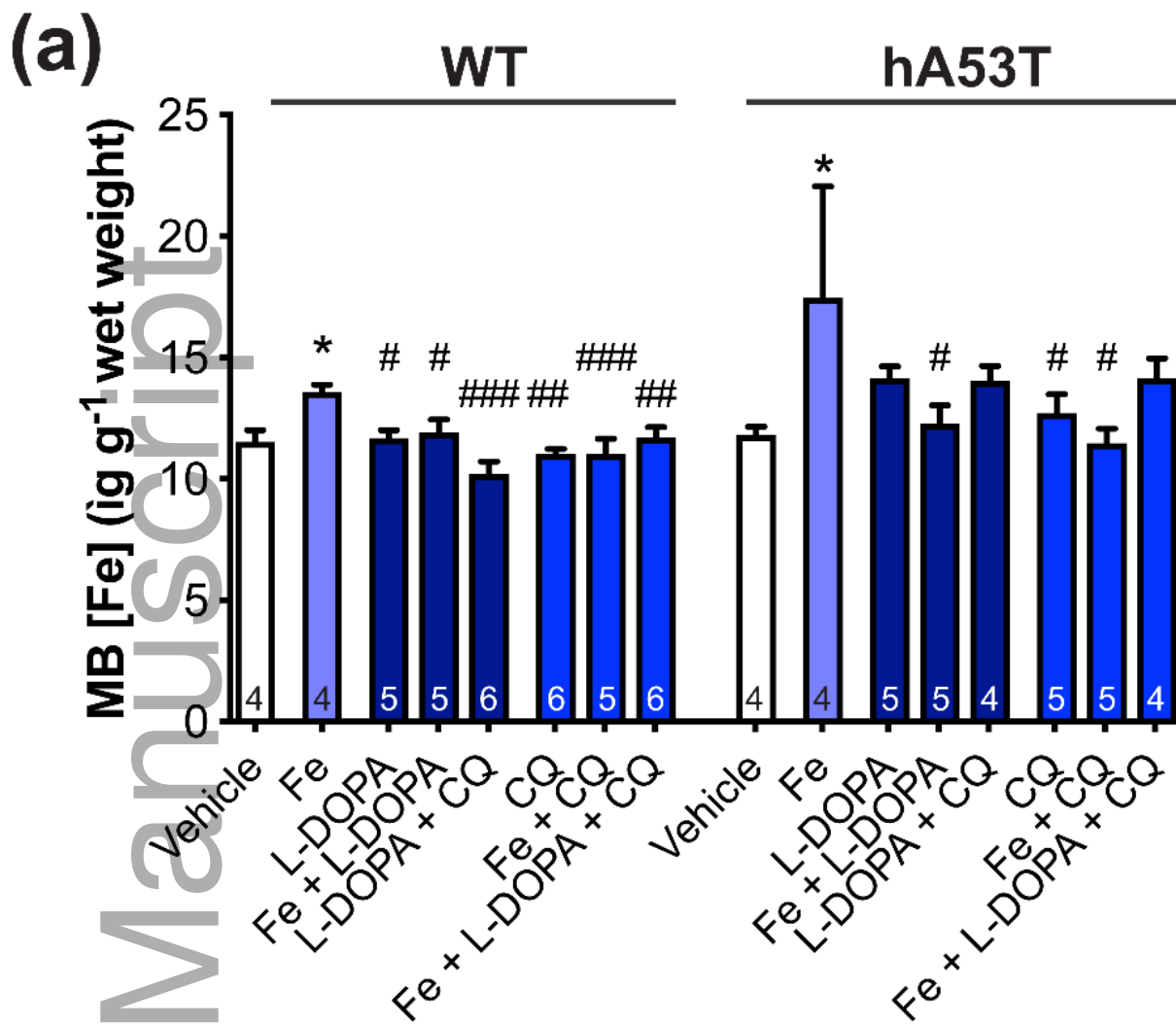


Author Manuscript

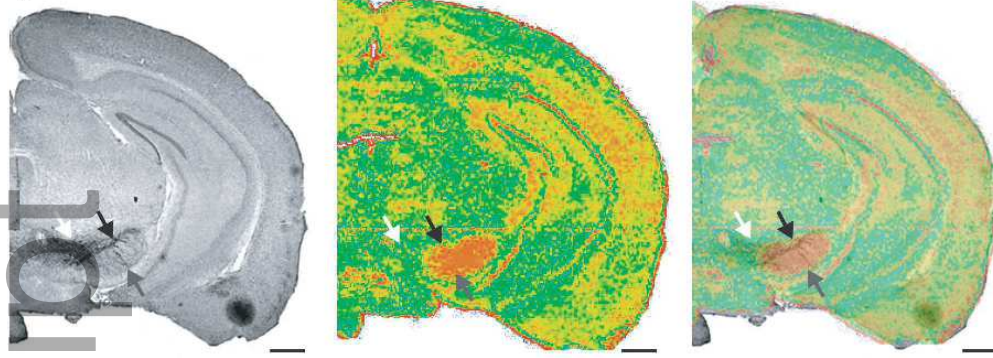


jnc\_14676\_f2.eps

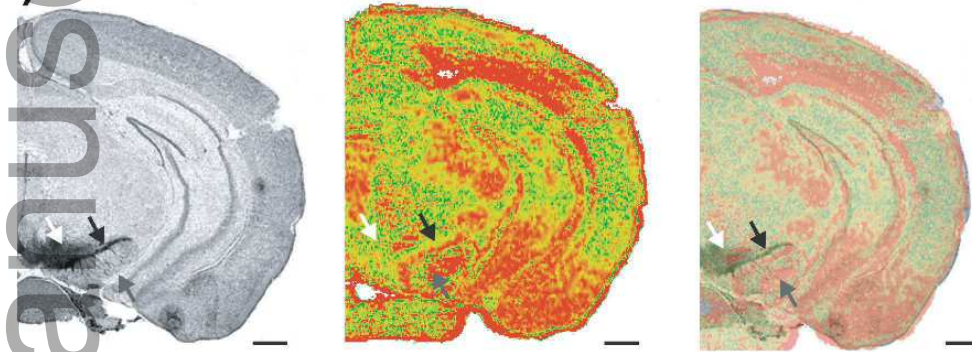




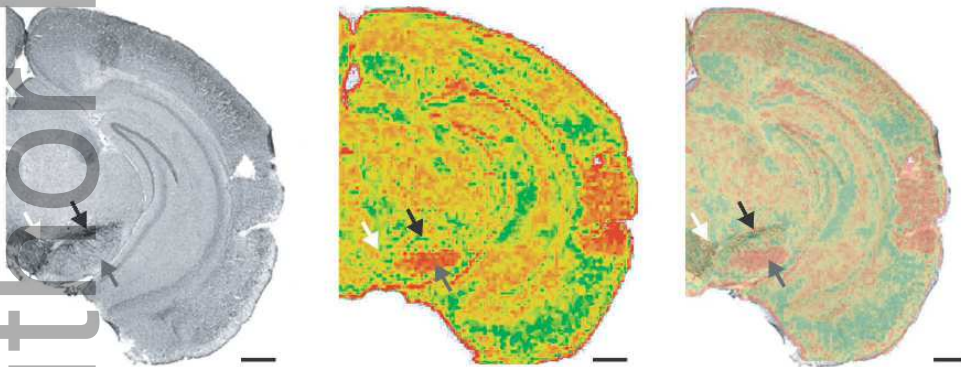
(a) Vehicle



(b) Fe

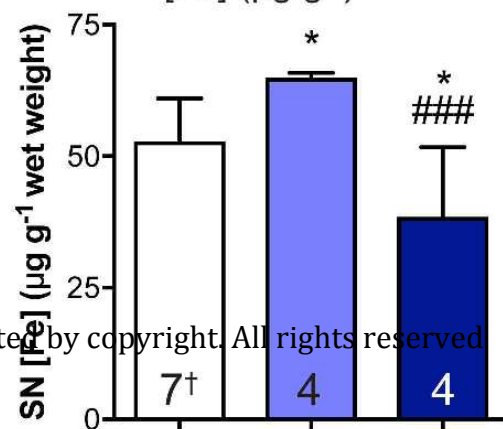


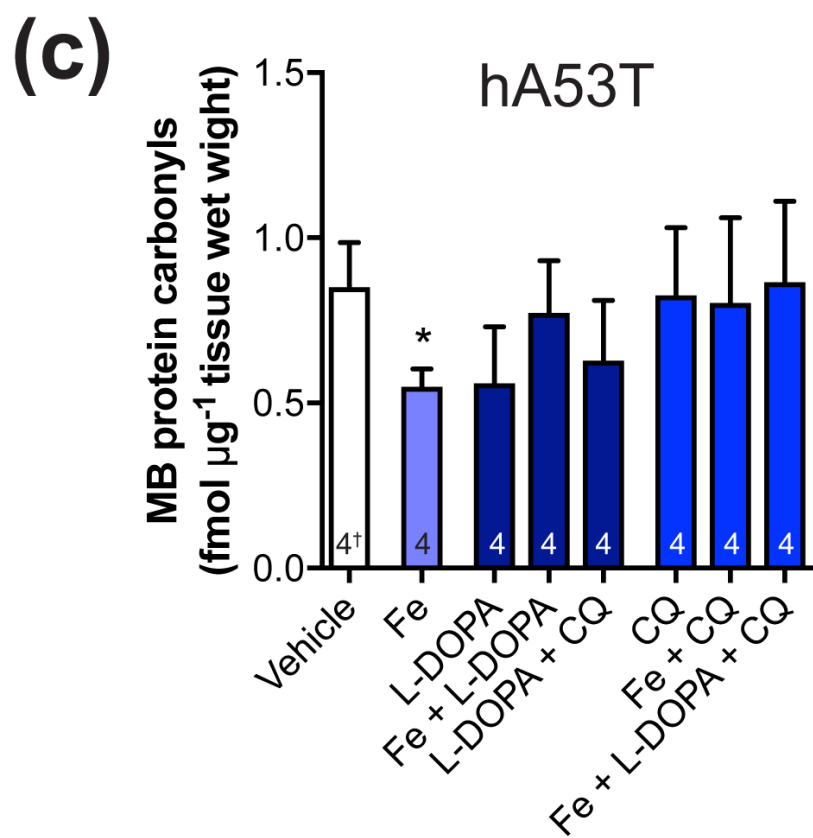
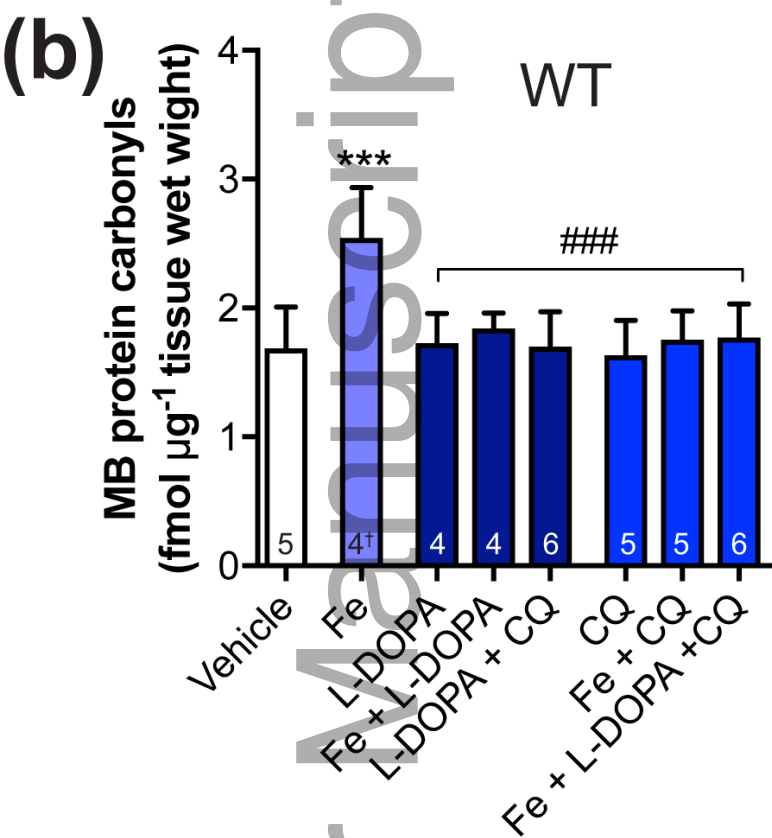
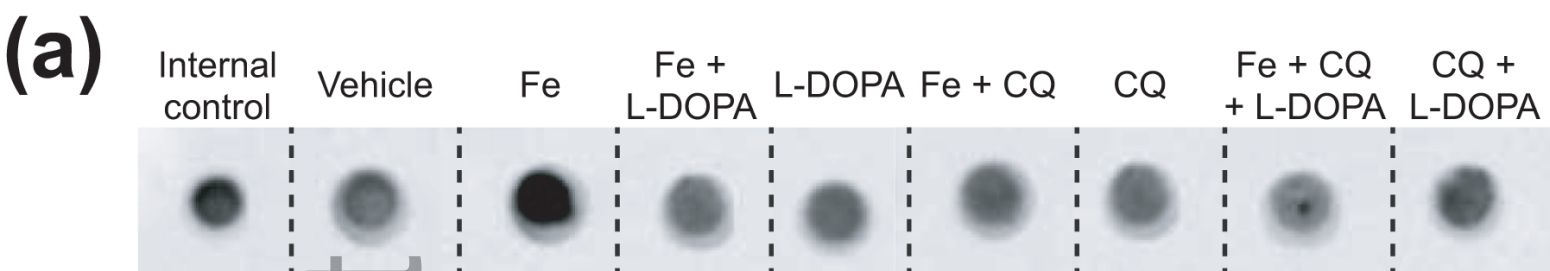
(c) Fe + L-DOPA



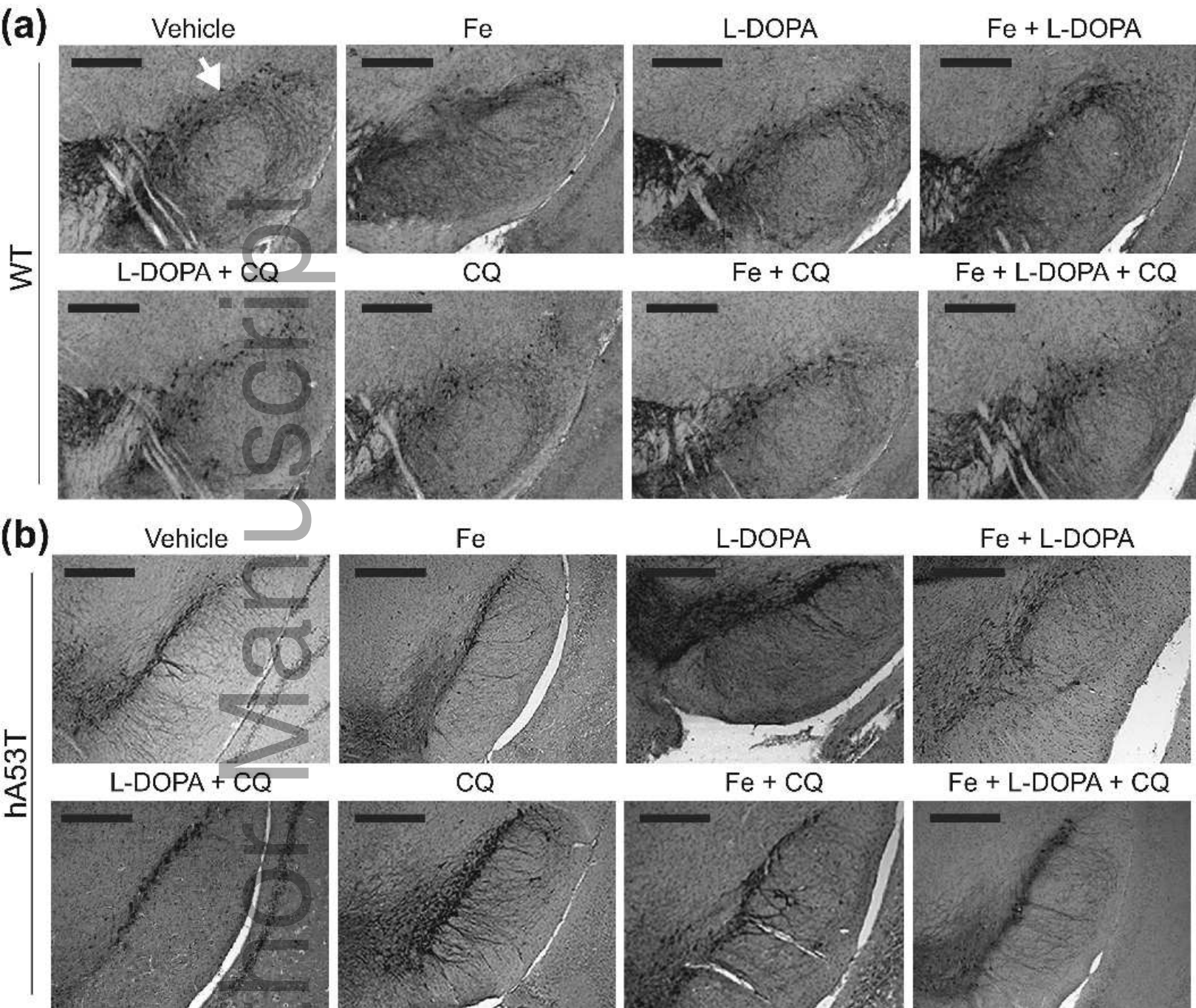
0 15 >30  
[Fe] ( $\mu\text{g g}^{-1}$ )

(d)

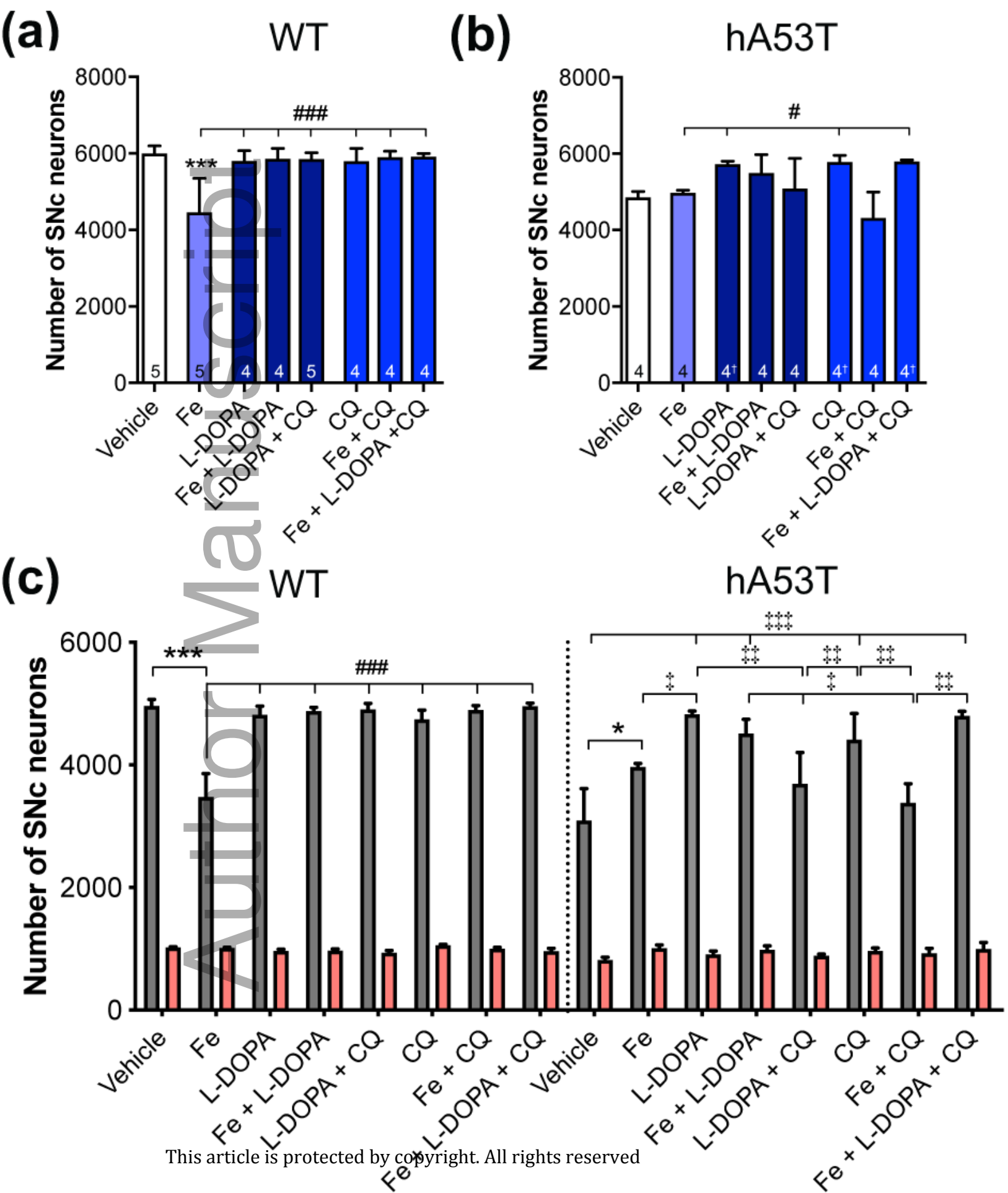


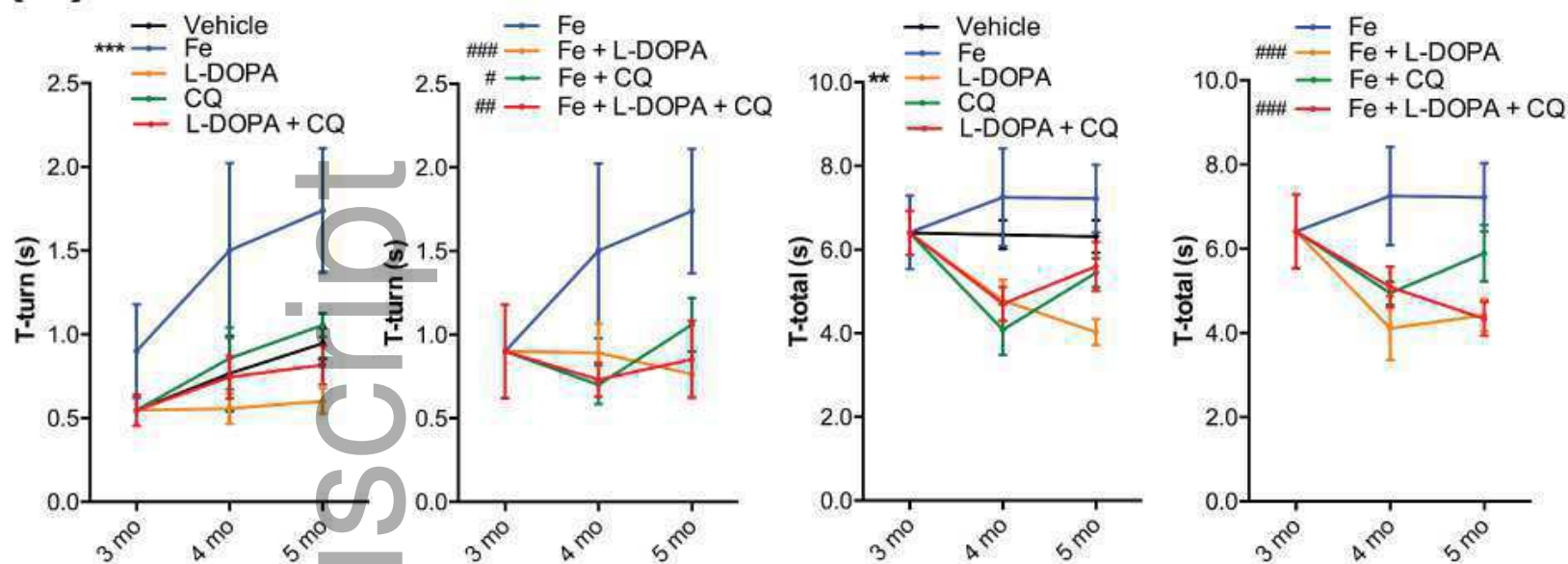
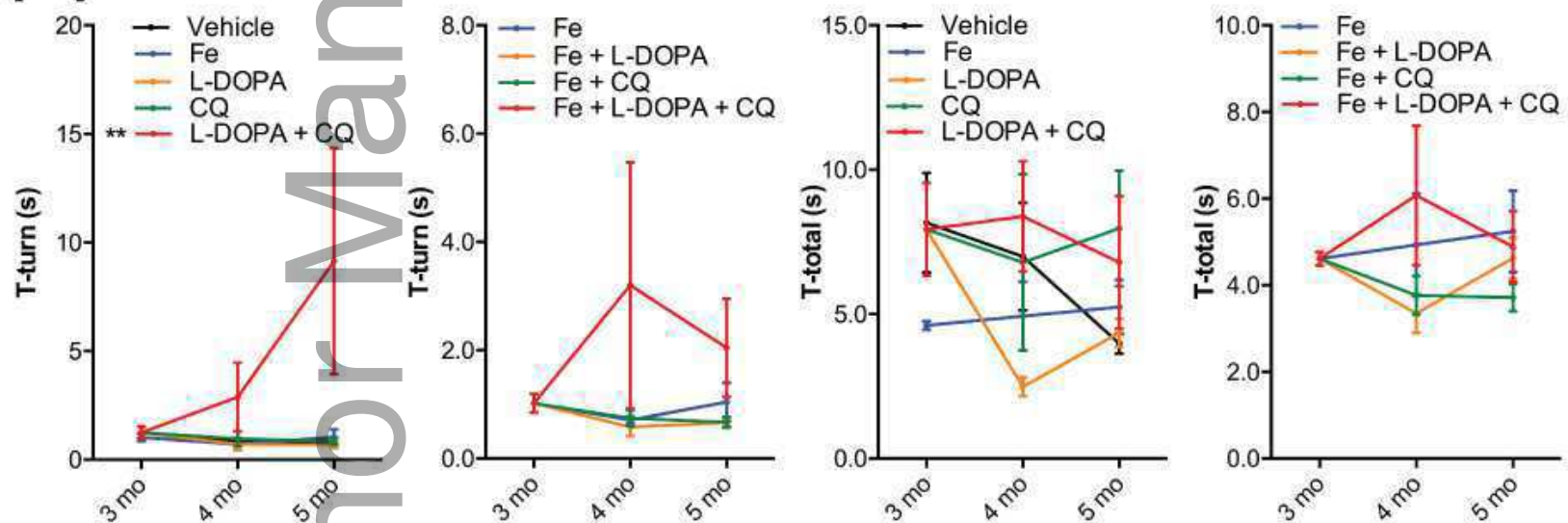


jnc\_14676\_f6.eps



jnc\_14676\_f7.eps



**(a)****WT****(b)****hA53T**

jnc\_14676\_f9.eps